University of Szeged
Faculty of Pharmacy
Institute of Pharmaceutical Analysis

Enantioselective high-performance liquid chromatographic separations utilizing *Cinchona* alkaloid- and polysaccharide-based chiral stationary phases

Ph.D. thesis

Gábor Németi

Supervisor:
Prof. Dr. István Ilisz, D.Sc.

2025

List of publications, presentations, and posters

Publications related to the thesis

I. **G. Németi**, R. Berkecz, S. Shahmohammadi, E. Forró, W. Lindner, A. Péter, I. Ilisz: Enantioselective high-performance liquid chromatographic separation of fluorinated *ß*-phenylalanine derivatives utilizing *Cinchona* alkaloid-based ion-exchanger chiral stationary phases: Enantioselective separation of fluorinated *ß*-phenylalanine derivatives
Journal of Chromatography A, 1670 (2022) 462974
https://doi.org/10.1016/j.chroma.2022.462974
if.: 4.1 (Q1 in analytical chemistry)

II. A. Bajtai, **G. Németi,** T. M. Le, Zs. Szakonyi, A. Péter, I. Ilisz: Enantiomeric separation of newly synthesized amino, thio, and oxy derivatives of monoterpene lactones, amides, and ester applying polysaccharide-based chiral stationary phases in normal-phase mode
Journal of Chromatography A, 1672 (2022) 463050
https://doi.org/10.1016/j.chroma.2022.463050
if.: 4.1 (Q1 in analytical chemistry)

III. **G. Németi**, R. Berkecz, T. M. Le, Zs. Szakonyi, A. Péter, I. Ilisz
High-performance liquid chromatographic enantioseparation of azole analogs of monoterpene lactones and amides focusing on the separation characteristics of polysaccharide-based chiral stationary phases
Journal of Chromatography A, 1717 (2024) 464660
https://doi.org/10.1016/j.chroma.2024.464660
if.: 3.8 (2023, Q2)
Sum if.: 12.0

Other publications

IV. A. Bajtai, Gy. Lajkó, **G. Németi**, I. Szatmári, F. Fülöp, A. Péter, I. Ilisz: High-performance liquid chromatographic and subcritical fluid chromatographic separation of α-arylated β-carboline, *N*-alkylated tetrahydroisoquinolines and their bioisosteres on polysaccharide-based chiral stationary phases
Journal of Separation Science, 42 (2019) 2779–2787
https://doi.org/10.1002/jssc.201900228
if.: 2.9 (2.878, Q2)

V. R. Berkecz, **G. Németi**, A. Péter, I. Ilisz: Liquid chromatographic enantioseparations utilizing chiral stationary phases based on crown ethers and cyclofructans
Molecules, 26 (2021) 4648–4866
https://doi.org/10.3390/molecules26154648
if.: 4.9 (4.927, Q2)

VI. J. P. Mészáros, **G. Németi**, J. M. Poljarevic, T. Holczbauer, N. V. May, É. A. Enyedy: Effect of the additional carboxyl group in half-sandwich organometallic 2,4-dipicolinate complexes on solution speciation and structure
European Journal of Inorganic Chemistry, 19 (2021) 1858–1868
https://doi.org/10.1002/ejic.202100122
if.: 2.6 (2.551, Q2)

VII. J. P. Mészáros, V. F. S. Pape, G. Szakács, **G. Németi**, M. Dénes, T. Holczbauer, N. V. May, É. A. Enyedy: Half-sandwich organometallic Ru and Rh complexes of (N,N) donor compounds: effect of ligand methylation on solution speciation and anticancer activity
Dalton Transactions, 50 (2021) 8218–8231
https://doi.org/10.1039/D1DT00808K
if.: 4.6 (4.569, Q1)

VIII. **G. Németi**, R. Berkecz, A. Péter, W. Lindner, I. Ilisz: *Cinchona* alkaloid-based zwitterionic chiral stationary phases applied for liquid chromatographic enantiomer separations: an updated overview
Book chapter of G.K.E. Scriba, ed., Chiral Separations, Springer New York, New York, NY, expected release in 2025

Total if.: 26.92

Presentations

I. **G. Németi**, S. Shahmohammadi, E. Forró, A. Péter, I. Ilisz: Investigation of enantioselective HPLC separations of fluorinated β^3-phenylalanine derivatives
27th International Symposium on Analytical and Environmental Problems; Szeged; Hungary; November 22–23; 2021

II. **G. Németi**, T. M. Le, Zs. Szakonyi, A. Péter, I. Ilisz: HPLC separations of *N*-azole compounds in polar organic and normal phase mode utilizing amylose-based chiral stationary phases
28th International Symposium on Analytical and Environmental Problems; Szeged; Hungary; November 14–15; 2022

III. **G. Németi**, D. Ozsvár, R. Berkecz, A. Péter, W. Lindner, I. Ilisz: Enantioselective separation of substituted amino acids utilizing *Cinchona* alkaloid-based chiral stationary phases
29th International Symposium on Analytical and Environmental Problems; Szeged; Hungary; November 13–14; 2023

Posters

I. **Németi G.**, Forró E., Fülöp F., Péter A., Ilisz I.: Fluorozott β^3-fenilalaninszármazékok folyadékkromatográfiás kölcsönhatásainak vizsgálata ioncserélő típusú királis állófázisokon
METT25; Egerszalók, Hungary, October 18–20, 2021

II. **G. Németi**, T. L. Minh, Zs. Szakonyi A. Péter, I. Ilisz: High-performance liquid chromatographic separations in polar organic and normal phase mode utilizing polysaccharide-based chiral stationary phases
33rd International Symposium on Chromatography; Budapest, Hungary, September 18–22; 2022

III. **G. Németi**, D. Ozsvár, R. Berkecz, P. Antal, W. Lindner, I. Ilisz: HPLC study of the enantioselective separation of β-methyl-substituted amino acids applying ion exchanger-based chiral stationary phases
13th Balaton Symposium on High-Performance Separation Methods; Siófok, Hungary; September 4–6, 2023

IV. **Németi G.**, T.M. Le, Szakonyi Zsolt, Péter Antal, Ilisz István
Pirimidinszármazékok folyadékkromatográfiás kölcsönhatásainak vizsgálata poliszacharid típusú királis állófázisokon
Elválasztástudományi Vándorgyűlés 2024; Visegrád-Lepence, Hungary; 2024. November 7–9.

Abbreviations and symbols

t_R	retention time
t_0	hold-up time
V_0	hold-up volume
k	retention factor, $k = (t_R - t_0)/t_0$
α	selectivity, $\alpha = k_2/k_1$, where 1: first- and 2: second-eluting peak
R_S	resolution, $R_S = 2 \times [(t_{R2} - t_{R1})/(w_1 + w_2)]$, w = peak width at the base of the peak
AA	amino acid
ABA	azole and benzoazole analogs of monoterpene lactone derivatives
(A)DMPC	(amylose) *tris*-dimethylphenylcarbamate
ATO	amino, thio, and oxy analogs of monoterpene lactone derivatives
CSP	chiral stationary phase
DEA	diethylamine
DMP	dimethylphenyl
EA	ethylamine
EEO	enantiomer elution order
FA	formic acid
FBP	fluorinated β^3-phenylalanine derivatives
PI(M)	polar ionic (mode)
NP	normal-phase
PO	polar organic
PS	polysaccharide
QD	quinidine
QN	quinine
RP	reversed-phase
SA	selectand
SO	selector
TEA	triethylamine
WAX	weak anion exchanger
WLR	weighted linear regression
ZIE	zwitterionic ion exchanger

Table of Contents

1. Introduction

In the world of pharmaceuticals, the concept of enantiomers holds great significance. Enantiomeric pairs, which are non-superimposable mirror images of each other, can exhibit strikingly different biological activities, influencing not only the effectiveness of a drug but also its safety profile. These mirror-image molecules can have varying interactions with biological systems, since various chiral compounds exist in living organisms, such as proteins, sugars, and enzymes. This discrepancy often leads to differences in therapeutic outcomes because of their different interactions. Furthermore, the desired pharmacological activity is often restricted to one of the enantiomers (eutomer), while the other enantiomer (distomer) may induce unwanted side effects or it can even be toxic during its metabolism. Chirality can be observed not only in pharmaceuticals but also in food additives, chirality can be observed (e.g., amino acids). These different effects of enantiomers emphasize the importance of synthesizing pure enantiomers or separating racemic (or scalemic) mixtures.

Various methods are available for the separation of enantiomers of chiral compounds. Liquid chromatography is the most widely used technique for enantiomeric separations due to its versatility in varying chromatographic conditions. The choice of stationary and mobile phases, which can greatly vary in polarity, plays a crucial role in the separation of analytes. The two members of the enantiomer pairs have the same physical and chemical properties. Consequently, their separation requires a chiral environment, where the enantiomers can form diastereomeric pairs with a selector through secondary interactions of different strengths. Direct chromatographic methods, especially when applying chiral stationary phases (CSPs), are the most often utilized techniques, since chiral columns with diverse selectors (SOs) are available on the commercial market. The interactions between the SO and the selectand (SA) can vary depending on the chromatographic environment (e.g., the solvation shell formed by the mobile phase) and the ligand attached to the silica backbone of the HPLC column.

2. Objectives

The primary objectives of this Ph.D. work were to achieve the liquid chromatographic separation of enantiomeric pairs of pharmacologically important compounds, as well as to investigate the mechanisms of interactions between the chiral SO and the SAs. These potential pharmaceutical agents are typically synthesized as a series of structurally related compounds with diverse functional groups, enabling the examination of differences in retention patterns due to the fine structural dissimilarities of both the SOs and SAs.

In order to assess the relationships between the molecular structure of different families of SOs and the chromatographic characteristics of the enantioseparation of various SAs, the main aims of this study are as follows:

- investigation of the effects of the mobile phase composition, focusing on the quality and ratio of the bulk eluent components, as well as the nature and concentration of acid and base eluent additives, on chromatographic parameters,
- comparative examination of the effects of variations in molecular structures on enantioseparations,
- exploration of the unique characteristics of the higher-order structure of the polysaccharide chains through the sequential application of diverse eluent compositions,
- thermodynamic characterization of enantioseparations by interpretation of the effect of temperature on chromatographic parameters.

3. Literature overview

3.1. Importance of chirality

Living organisms often display different responses to the enantiomers of chiral compounds such as drugs, agrochemicals, food additives, and fragrance materials. Because of their identical physical and chemical properties, strong demand has arisen in both the life and pharmaceutical sciences for analytical tools to separate individual stereoisomers. Due to their characteristics, the separation of enantiomers requires a chiral environment to form diastereomeric pairs with the so-called SO, which provides the stereospecific chemical interactions between the enantiomers and the SO required for separation [1].

3.2. Choices of enantioselective separations

A plethora of techniques, for example, gas chromatography, supercritical fluid chromatography, biotransformation, asymmetric synthesis, membrane techniques, etc., can be chosen to separate and/or analyze enantiomeric mixtures. However, liquid chromatographic techniques are one of the most often applied methods, because of their versatility and the availability of a wide range of selectors and columns, which make them appealing, either for analytical or industrial scale. It is feasible to apply homochiral reagents as SOs in the mobile phase, with the use of an achiral column, or make functionalized SAs via derivatization reactions if the compounds have reactive functional groups. However, the use of an SO dissolved in the mobile phase has lost its practical importance in HPLC, because its main field of application is currently capillary electrophoresis. Nowadays, direct enantioselective chromatographic methods apply chiral stationary phases (CSPs), where the selector, in most cases, is attached covalently to silica gel. [2–4].

Considering instrumentation, the same system, including detection, can be used for chiral columns as for achiral columns, enabling simple changes between chiral and non-chiral methods. Polarimeter and circular dichroism detectors can also be used in chiral HPLC systems, providing additional information on the configuration of the analytes.

To further enhance the performance of an HPLC system, CSPs can be coupled to achiral and/or chiral columns, either as a tandem column or as an additional dimension

to form a multidimensional LC system, which is often coupled with a mass spectrometer [5,6].

3.3. Chiral HPLC columns (CSPs)

Tswett introduced chromatographic adsorption analysis at the beginning of the 1900s but faced skepticism and rejection [7]. In the 1930s, the rediscovery of chromatography highlighted its considerable potential, ultimately allowing it to be widely adopted and awarded numerous Nobel Prizes for its research [8].

The first chiral stationary phase was described in 1939, when partial separation of enantiomers was reported by *Henderson* and *Rule*, using a lactose-filled chromatographic column [9]. Due to the advancement of paper and column chromatography, innovations in the field of liquid chromatography in the 1980s led to the development of HPLC equipments and packed columns. Highly efficient CSPs started to disseminate, and porous silica particles with small diameters and high mechanical stability established the progression of modern CSPs. By the end of the 1990s, more than 1000 CSPs have been existed for HPLC and GC, and more than 200 were commercially available. Since then, both the number of new CSPs and SOs and the demand for new ones have increased [10].

The separation of enantiomers is based on the temporary formation of diastereomeric pairs through the interactions between the SAs and the SO. A widely accepted model developed by *Easson* and *Stedman* in 1933 explains the different biological effects of chiral compounds with a so-called three-point-interaction model (**Figure 1**) based on the interaction of stereoactive drugs with receptors [11]. Reports have been made of the enantioseparation of several amino acids (AAs) and other small chiral compounds by paper chromatography in the early 1950s [12,13]. *Dalgliesh* applied the previous three-point interaction model for the interpretation of structure-interaction relationships of the separation of AAs on the cellulose SO.

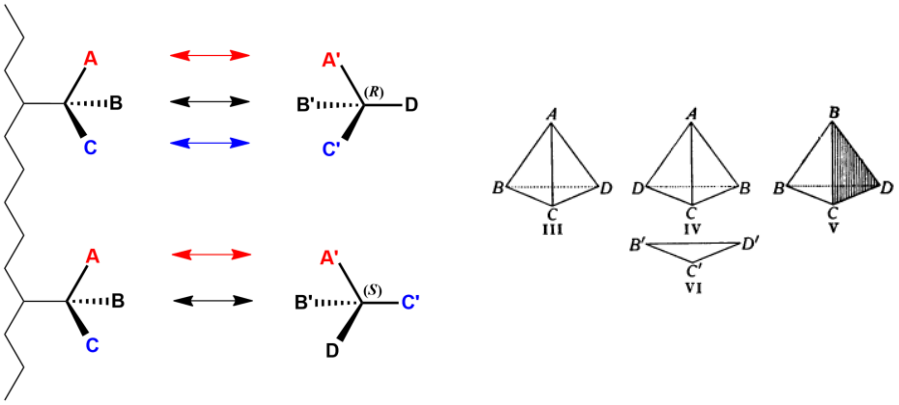

Figure 1. Schematic representation of the three-point-interaction model (on the left) and the first depiction of the model in the case of chiral drugs and a receptor (on the right, [11])

Until this point in time, all three interactions were considered attractive. *Pirkle* and *Pochapsky* [14] as well as *Davankov* [15] improved the model, highlighting that at least one of the three interactions must be stereoselective. Furthermore, not only attractions but steric effects as repulsions are also should be considered. The stability of these diastereomeric SA–SO complexes is driven by the strength of non-covalent interactions. Moreover, these compounds are solvated, thus, the environment of the interactions is greatly affected by the mobile phase composition [3].

Overall, there are several possible types of interaction types during the formation of the SA–SO complexes:

- electrostatic attraction or repulsion
- π–π
- hydrogen bonding
- polar
- steric

Ionic interactions are fairly strong, non-directional, and long-ranged; therefore most likely occur in a non-stereoselective manner. On the contrary, π–π interactions, hydrogen bonding, and dipole stacking are only significant if the binding geometries of the SO and SAs more or less complement each other. This fitting of close-range interaction sites likely leads to chiral discrimination [3,16].

The SOs of CSPs could be grouped by their origin, such as natural, semi-synthetic, and synthetic. However, today's CSPs are mostly semi-synthetic, since natural SOs are modified to enhance their efficacy, and synthetic ones are often based on structures that naturally occur. It is more expedient to group them by their structure or nature,

considering that the same family of structures is responsible for the same primary interactions. These include [17]:

- ion exchangers
- oligosaccharides, e.g., cyclofructans, cyclodextrins
- polysaccharides (PSs)
- proteins, peptides, AAs, e.g., ligand exchangers, π-complex selectors
- macrocyclic molecules
- molecularly imprinted polymers

Results presented in my doctoral dissertation are derived from the utilization of *Cinchona* alkaloid-based and PS-based columns, hence, the key properties of these CSPs will be discussed in the following sections.

3.3.1. Cinchona alkaloid-based CSPs

Cinchona alkaloids are the basis of one of the most popular chiral ion exchanger stationary phases. The two most common alkaloids related to chiral separations are quinine (QN) and quinidine (QD). As extensively outlined in the paper by *Lämmerhofer* and *Lindner* [18], the first description of the application of *Cinchona* alkaloids for enantiomeric resolution by LC dates already back to the early 1950s [19,20]. QN was first used in the early 1980s for chiral separations as counterion [21]. In 1985, *Rossini et al*. created the first QN-based CSP, with quinine covalently attached to silica gel [22]. However, this CSP suffered from low enantioselectivities and a narrow application range. In the late 1990s, *Lindner* and his co-workers first introduced C-9 carbamate-bonded (through a thioether linker) QN- and QD-based selectors for one extra H bonding and/or dipole–dipole interaction site. Note, that the selectors already had the quinolone ring and the ion pairing site of the quinuclidine group capable of π-basic and steric interaction. These QN- and QD-based columns are often referred to as "pseudo-enantiomers" because they behave as quasi-enantiomers. The elution order of the enantiomers should have to change when the column has changed to their other pair of quinuclidine stationary phase. The authors actually observed this phenomenon [23]. Three years later, they changed the binding site of the silica to the vinyl group besides the quinuclidine group (through a C-11 thioether linker), and modified the hydroxy group at C-9 to a *tert*-butyl carbamate group, keeping the role of the carbamate group, while adding a new steric interaction site via the *tert*-butyl group [24]. With this improvement, the enantiodiscrimination ability of

the weak anion exchanger (WAX) SOs, namely QN–AX and QD–AX, has increased markedly and these CSPs have become popular, even nowadays [25]. Development of these columns is still ongoing. Nowadays the main focus in column development is to increase efficiency by the introduction of core–shell-type WAX columns [26].

There is another significant evolutionary path of these CSPs, which has resulted in a new type of ion exchanger CSPs, i.e., the incorporation of enantiomerically pure *trans*-2-aminocyclohexylsulfonic acid [(*S*,*S*)- or (*R*,*R*)-ACHSA], a strong cation exchanger group onto the carbamate group, instead of the previous *tert*-butyl group applied before. The resulting CSPs can act as chiral anion and cation exchangers but also as zwitterionic ion exchangers (ZIE) through double electrostatic interactions occurring simultaneously with ampholytic analytes, as illustrated in **Figure 2**. These new CSPs are **ZWIX(–)** and **ZWIX(+)** [18].

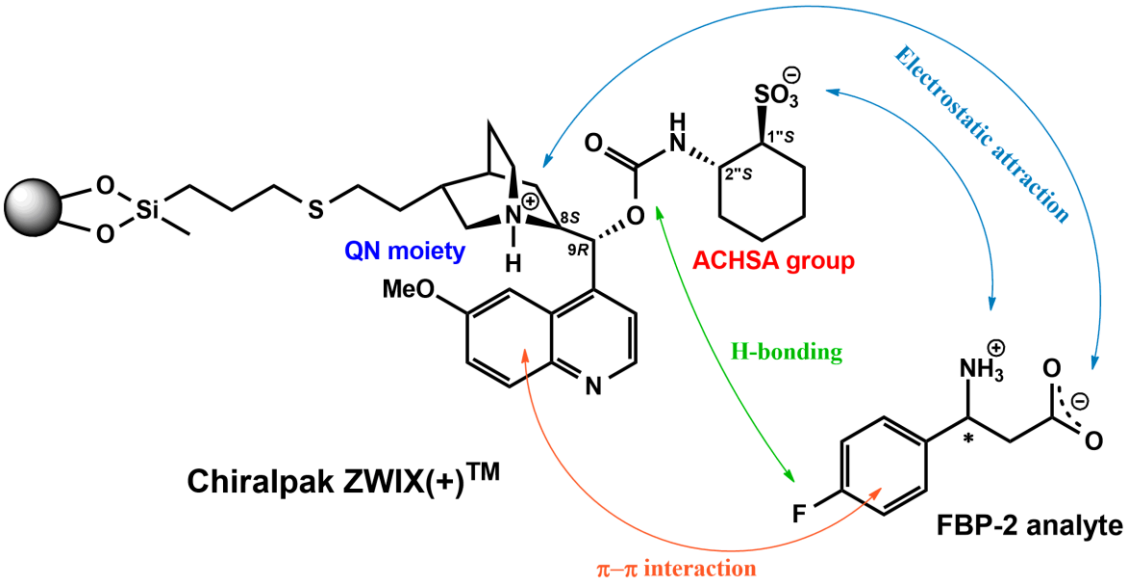

Figure 2. The structure and some possible interactions between the zwitterionic CSPs (with both anion and cation exchanger sites) and the **FBP–2** fluorinated β^3-phenylalanine

Ion pairing and ion exchange are the main driving forces of the retention as a strong and long-ranged force in the case of cationic, anionic, and zwitterionic-type SOs. Adding acid and base modifiers into the mobile phase, they form counterions, and these act as competitors for the SA and SO ionic functional groups. In the case of zwitterionic SOs, both cations and anions can be considered as counterions. Furthermore, the two ionizable functional groups on the SO also act as counterions. This way the zwitterionic retention mechanism is less affected by the concentration of counterions, but still, the retention can

be controlled to an extent [27,28]. Moreover, enantioseparations can even be realized without additives [29].

3.3.2. Polysaccharide-based CSPs

As mentioned earlier, paper chromatography was the first field of separation techniques that applied PS-based selectors for separating enantiomers of AAs and various analytes, following with other compounds [12,13]. Only a few years later, in 1956, *Krebs et al*. reported the first successful (partial) enantioseparations of several mandelic acid derivatives and various AA derivatives on a natural starch-filled liquid chromatographic column [30]. Investigations of chromatographic applicabilities of PS-based CSPs started to increase, with *Hesse* and *Hagel* separating the enantiomers of Tröger's Base on cellulose triacetate-based columns and thin layer chromatography plates in 1973 [31].

However, the low stability of PSs, whether due to physical or chemical factors, was still a problem, *Okamoto et al*. resolved it in 1984 [32]. First, they adsorbed cellulose-triacetate on the surface of silica gel and found a different behavior when separating the enantiomers of Tröger's Base in comparison to *Hesse*'s microcrystalline CSPs. Their newly synthesized SOs based on various PSs besides today's cellulose- and amylose-based preparations, such as chitosan, xylan, curdlan, dextran, and inulin. Their SOs were modified with phenyl groups, were attached to the saccharides via urethane bonds (making phenylcarbamate functional groups), and converted almost all hydroxy groups. Good enantioseparations were reported using normal phase chromatographic mode [32]. The performance of these selectors was tested and improved with more than 30 different electron-donating or electron-withdrawing groups on the phenyl ring in different positions and numbers. The next great improvement was when the SO was attached to the silica backbone via covalent bonds that became popularized in the early 2000s. The main advantage of the immobilized-type columns is their high stability—their physical and chemical stability is close to that of the silica backbone [33].

As a result of the ease of preparation, the coated phases were initially commercialized. Their disadvantageous property is their incompatibility with some solvents (e.g., tetrahydrofuran, ethyl acetate, *tert*-butyl ether, chlorinated solvents, etc.), which may dissolve or swell the PS coating, drastically reducing or even killing the efficiency of the column. By covalently immobilizing the PS SO onto the surface of the silica support, this limitation factor could be eliminated, and any standard or non-standard

solvent became available as a mobile phase component or neat solvent. This means that these CSPs can work in normal-phase mode (NPM), polar organic mode (POM), polar ionic mode (PIM) (as acid and/or base additives can cause major changes in the chromatographic parameters [34–36]), reversed-phase mode (RPM), and in sub/supercritical fluid chromatography (SFC) as well [33,37]. The applied mobile phases are often compatible with mass spectrometry (MS). Moreover, hydrophilic interaction liquid chromatography (HILIC)-like behavior was reported in several cases [35,38–40]. The application field of PS-based CSPs further increased until it became the most common type of chiral columns in enantioselective liquid chromatography [41]. Although both the coated and immobilized CSPs have the same SOs, they could have markedly different chromatographic behavior due to the differences in their higher-order structures and points of attachments to the silica backbone, which could lead to different enantiorecognition or even cause reversed enantiomer elution orders (EEOs) [42,43]. Structures of the PS-based CSPs utilized in my research work are shown in **Figure 3**.

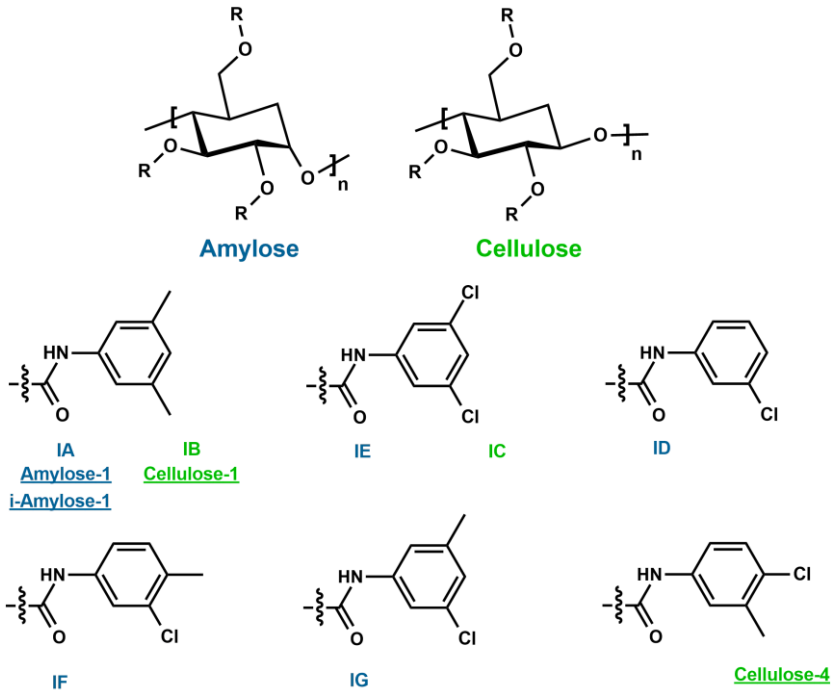

Figure 3. Structures of the amylose and cellulose chains and the modifier phenylcarbamate groups of the utilized **Daicel** and **Phenomenex** columns

The outstanding performance of these columns originates from the diverse functional groups and structural arrangement of the polymer chains: i) molecular chirality arises from the presence of multiple stereogenic centers of the glucopyranose units, ii) the helical (in the case of amylose) or linear (in the case of cellulose) polymer chain

yields conformational chirality, and iii) supramolecular chirality provided by the arrangement of polymer chains relative to each other. H-bonding and dipole–dipole interactions are crucial for chiral recognition. H-bonding and dipole interactions primarily involve the carbamate group, whereas π–π interactions are associated with the phenyl group and they can additionally stabilize the SA–SO complex [3].

3.3.2.1. Hysteretic behavior of polysaccharide-based CSPs

As mentioned earlier, multimodality is a very appealing trait of the PS-based CSPs. However, despite numerous studies on the enantiorecognition mechanism of PS-based CSPs, an important phenomenon, i.e., their hysteretic behavior, has only been described very recently [44–47]. Zhang and Franco mentioned changes in column selectivity when applying non-standard solvents in the case of Chiralpak IA, the first commercially available immobilized column [48]. They explained the phenomenon with a change in the supramolecular structure of the polymeric chains. Recently, *Horváth* and *Németh* provided several examples of the history-dependent retention behavior in the case of selectors based on amylose *tris*-(3,5-dimethylphenylcarbamate) (ADMPC) [44]. As a realistic explanation, a hindered transition of the higher-order structure of the ADMPC selector accounted for the observed hysteresis effects. Later, the same authors [45–47] and others [49,50] reported more examples of how the eluents used previously on a particular column affect column performance. Similar phenomena were observed in two cases, where hysteretic behaviors were induced by temperature changes [51,52]. Based on these findings, the hysteretic behavior seems to be a more general characteristic, at least for amylose-based CSPs.

3.4. Thermodynamic equations related to chiral separations with HPLC

Chiral LC enantioseparations tend to be more sensitive to changes in temperature compared to achiral LC. Therefore, it is crucial to investigate the temperature dependence and thermodynamic properties that characterize the separation of chiral isomers.

Selectivity often decreases with increasing temperature during the separation of enantiomers, since the temperature-dependent distribution of the components (enantiomers) between the stationary and mobile phases could be different. This is known as the thermodynamic effect, which is complemented by the temperature dependence of the equilibrium constants of the SO–SA complexes. In contrast, the eluent has lower viscosity at elevated temperatures, leading to an increased diffusion constant that

enhances the separation by faster mass transfer between the SO and the mobile phase. This kinetic effect is the opposite of the thermodynamic effect. Consequently, the outcome of the separation is dependent on the balance of these opposing effects and must be empirically determined for each case (whereas there are computer-based calculations utilizing different models in this area, their applicability is rather limited [53]).

The driving force of an enantiomeric separation is the difference in the *Gibbs energy* between the two SO–SA complexes during the process of adsorption. The relation of the standard *Gibbs energy* to the complexation equilibrium constant *K* of the SO–SA complexes can be described with the following equation, combined with the *Gibbs–Helmholtz equation*:

$$\Delta G^0 = \Delta H^0 - T\Delta S^0 = -RTlnK \quad (1)$$

$$\ln K = -\frac{\Delta H^0}{RT} + \frac{\Delta S^0}{R} \quad (2)$$

where ΔG^0 is the standard change of *Gibbs energy*, ΔH^0 is the standard change of enthalpy, ΔS^0 is the standard change of entropy, R is the universal gas constant, and T is the absolute temperature in Kelvin. The retention factor (k) can be expressed by multiplying the equilibrium constant with the phase ratio:

$$k = K\phi = K\frac{V_s}{V_m} \quad (3)$$

where ϕ is the phase ratio (in the dissertation, I use the phase ratio as the reciprocal of the IUPAC recommendation), V_s is the volume of the stationary phase, and V_m is the volume of the mobile phase.

The *van't Hoff* equation, which interprets the dependence of *ln k* vs. T^{-1}, can be obtained by the combination of **Eqs. (2)** and **(3)**:

$$\ln k = -\frac{\Delta H^0}{RT} + \frac{\Delta S^0}{R} + \ln\phi \quad (4)$$

The phase ratio is unknown in most cases, and it is difficult to measure it correctly, and it even could change depending on the chromatographic environment (e.g., temperature, mobile phase composition) [54–56]. The equilibrium constant can be expressed separately for the second- (K_2) and first-eluting (K_1) enantiomers. Then these are substituted into **Eq. (1)** as the difference of the standard *Gibbs energies* of the two chiral antipodes:

$$\Delta(\Delta G^0) = \Delta G_2^0 - \Delta G_1^0 = \ln\frac{K_2}{K_1} \quad (5)$$

The phase ratio is the same for both enantiomers and since selectivity is $\alpha = k_2/k_1$, this way the combination of **Eqs. (5)** and **(3)** results in the form of the *van't Hoff* equation without the phase ratio:

$$\ln \alpha = -\frac{\Delta(\Delta H^0)}{RT} + \frac{\Delta(\Delta S^0)}{R} \quad (6)$$

Due to the limitations of the *van't Hoff* equation – such as not considering different binding sites, assuming non-changing heat capacity in the temperature range of measurements, being sensitive to outlier data, etc. – only apparent thermodynamic parameters can be obtained. Nevertheless, valuable theoretical and practical assumptions can be made for the better understanding of chiral separation mechanisms [37,56].

3.5. Evaluation of thermodynamic data and determination of confidence intervals

To decrease sensitivity to outliers, the ln α (and ln k) vs. T^{-1} curves were evaluated based on weighted linear regression (WLR). The weighting variable of the seeming outlier data points was reduced to obtain more accurate mean values and confidence intervals. The WLR and confidence intervals (at a confidence level of 95%) were calculated with Microsoft Excel 2016 using the Real Statistics Resource Pack Add–In. Since the free energies were calculated from enthalpy and entropy parameters, their confidence intervals were calculated by taking the propagation of error into account [57,58].

3.6. Importance of the investigated analytes

3.6.1. Fluorinated β³-phenylalanine derivatives

Many chiral compounds are involved in processes that take place in living organisms. Typically, only one enantiomer of the image–mirror image pairs of chiral molecules dominate in nature, such as the L-enantiomers in the case of AAs. On one hand, the two members of the enantiomer pairs may have significantly different biological effects and, consequently, it is important to either synthesize the pure enantiomers or separate racemate mixtures. Let me therefore note here that D-amino acids are also present in living organisms, and they can be, e.g., biomarkers of musculoskeletal diseases [59], or D-phenylalanine could serve as a potential therapeutic agent for inhibiting amyloid formation in phenylketonuria caused by L-phenylalanine [60]. *β*-AAs also play important roles in Humans [61]. *β*³-AAs have an additional methylene

group between the carboxyl and amino groups. The number 3 marks the attachment point of the substituent to the base amino acid chain (in the case of β^3-phenylalanine, both the phenyl ring and the amino group connect to the same C atom).

Studying the bioactivity of drugs after the replacement of certain atoms or functional groups with fluorine became an intensively researched topic in the second half of the last century. Fluorine-containing active ingredients were only present in 2% of pharmaceutical medicines in the 1970s, while it can be estimated at around 25% nowadays [62]. Incorporation of fluorine can alter many of the properties of the compounds, such as the kinetic profile, steric interaction of the functional groups, lipophilicity or the ability to make H-bridge interactions, thus increasing the efficacy of a drug by orders of magnitude [63].

Application of a CSP-based chromatographic technique is a useful tool to determine the low amount of AA enantiomers as biomarkers [64].

3.6.2. Monoterpene lactone derivatives

Compounds with lactone and amide skeletons can have various types of biological activity. For example, the α-methylene-γ-lactone moiety, which is the key structural feature of numerous natural terpenoids, acts as a Michael acceptor, and it reacts with nucleophiles in enzymes, transcription factors, and other proteins, alkylating them irreversibly [65]. Loliolides, even without the α-methylene group, have promising anti-hepatocellular carcinoma [66,67], neuroprotective, and anti-inflammatory therapeutic effects [68]. These terpenes typically have poor water solubility and, therefore, they transform a parent bioactive natural compound to a new and more bioactive one. The method is a semi-synthetic approach by the incorporation of heteroatoms (N, O, or S), which could enhance aqueous solubility, and it improves the pharmacokinetic profile, maintaining or even augmenting the biological activity of the parent molecule [69]. Heterocyclic compounds are also of paramount interest in medicinal chemistry. Among them, imidazoles and triazoles, as well-known five-membered heterocyclic ring systems, have important properties in various medicinal agents [70]. Benzimidazole ring systems can be found in several proton-pump inhibitors against peptic ulcer and gastroesophageal reflux, in antibiotics and, in addition, they showed in vitro antiprotozoal activity [71].

Since biological activities of lactone analogs, in many cases, depend strongly on their stereochemistry, there is a need for analytical methods to determine the enantiomeric purity of lactones and their derivatives.

4. Experimental

4.1. Chromatographic systems

Measurements were carried out on two HPLC systems:

The first is a Waters Breeze system consisting of a 1525 binary pump, a 2996 photodiode array detector, a 717 plus autosampler, and the Empower2 data manager software (Waters Corporation, Milford, MA, USA). The chromatographic system was equipped with a Rheodyne Model 7125 injector (Cotati, CA, USA) with a 20-μL loop. The columns were thermostated in a Lauda Alpha RA 8 thermostat (Lauda Dr. R. Wobser GmbH & Co. KG., Lauda–Königshofen, Germany). The precision of temperature adjustment was ±0.1 °C.

The second HPLC system is a Shimadzu Prominence HPLC system (Shimadzu Corporation, Kyoto, Japan) equipped with a CBM–20A system controller, a DGU–20A solvent degasser, an LC–20AB binary pump, an SPD–M20A photodiode array detector, a CTO–20AC column oven, and a SIL–20AC autosampler. Lab–Solution chromatography data software (Shimadzu Corporation, Kyoto, Japan) allowed the acquisition and processing of chromatographic data.

4.2. Applied chiral HPLC columns

4.2.1. Cinchona alkaloid-based chiral ion exchangers

Chiralpak **ZWIX(+)** and **ZWIX(−)** columns (150 × 3.0 mm ID, 3 μm particle size for both columns) and QN–AX, QD–AX columns (150 × 4.6 mm ID, 5 μm particle size for both columns) were from Chiral Technologies Europe (Illkirch, France). The hold-up times (t_0) of the columns were determined by injecting 1% acetone mixed with MeOH at each investigated temperature and eluent composition. The flow rate was set at 0.6 mL min^{-1} and the column temperature at 25 °C, if not stated otherwise.

4.2.2. Polysaccharide-based chiral stationary phases

Their structures can be seen on **Figure 2**. The hold-up times (t_0) of these columns were determined by injecting the solution of tri-*tert*-butyl benzene (TTBB) at each investigated temperature and eluent composition. TTBB shows retention under RP conditions [56], thus pure 2-PrOH or MeOH was also injected in all cases when any

amount of H_2O was present in the mobile phase and, in most cases, for other mobile phases as well, to test the retention of TTBB.

4.2.2.1. Coated-type CSPs

The utilized coated-type CSPs were: Lux Amylose-1 (**cA1**) with amylose *tris*-(3,5-dimethylphenylcarbamate) selector, Lux Cellulose-1 (**cC1**) with cellulose *tris*-(3,5-dimethylphenylcarbamate) selector and Lux Cellulose-4 (**cC4**) with cellulose *tris*-(4-chloro-3-methylphenylcarbamate) selector. All columns have the same physical characteristics (250 × 4.6 mm ID, 5 μm particle size, Phenomenex, Torrance, CA, USA).

4.2.2.2. Immobilized-type CSPs

Immobilized-type CSPs listed below were also studied. The Lux i-Amylose-1 (**iA1**) with amylose *tris*-(3,5-dimethylphenylcarbamate) selector (250 × 4.6 mm ID, 5 μm particle size) was from Phenomenex (Torrance, CA, USA). The HPLC columns from Daicel were Chiralpak IA (**IA**) with amylose *tris*-(3,5-dimethylphenylcarbamate) selector, Chiralpak IB (**IB**) with cellulose *tris*-(3,5-dimethylphenylcarbamate) selector, Chiralpak IC (**IC**) with cellulose *tris*-(3,5-dichlorophenylcarbamate) selector, Chiralpak ID (**ID**) with amylose *tris*-(3-chlorophenylcarbamate) selector, Chiralpak IE (**IE**) with amylose *tris*-(3,5-dichlorophenylcarbamate) selector, Chiralpak IF (**IF**) with amylose *tris*-(3-chloro-4-methylphenylcarbamate) selector, and Chiralpak IG (**IG**) with amylose *tris*-(3-chloro-5-methylphenylcarbamate) selector. All columns have the same physical characteristics (250 × 4.6 mm ID, 5 μm particle size, Chiral Technologies Europe, Illkirch, France).

4.3. Chemicals

Methanol (MeOH), acetonitrile (MeCN), abs. ethanol 99.8% (EtOH), 1-propanol (1-PrOH), 2-propanol (2-PrOH), 1-butanol (BuOH), and *n*-hexane were of HPLC gradient grade. Ethylamine (EA), diethylamine (DEA), triethylamine (TEA), triethanolamine (TEOA), and formic acid (FA) of analytical reagent grade were purchased from VWR International (Radnor, PA, USA).

4.4. Studied analytes

The studied analytes can be grouped into three categories: fluorinated β^3-phenyalanines (**FBP**), amino, thio, and oxy analogs of monoterpene lactone derivatives (**ATO**), and azole and benzoazole analogs of monoterpene lactone derivatives (**ABA-**). At least one of the two enantiomers ("A" and/or "B") was available in enantiomerically pure form (enantiomeric excess > 99%) for each analyte (in the case of **FBP**: A and racemic mixture; **ATO** and **ABA**: A and B were available). The synthesis of analytes **FBP** [72], **ATO** and **ABA** [73] can be found in previous articles and their supporting information. Complete structures can be seen in the original publications this thesis related to, with the majority of the analytes being first examined in these publications [74–76]. Results were obtained under different chromatographic conditions for **FBP–1** and **2** with a crown ether-based CSP [77], and macrocyclic glycopeptide-based CSPs [78], for **FBP–1** with ZIE-based CSPs [79]; and for **ATO–1** and **7** with PS-based CSPs [43] published earlier, while for all **FBP** analytes with macrocyclic glycopeptides were published later [80]. The structures of the "A" configurations of the investigated analytes are shown in **Figure 4**.

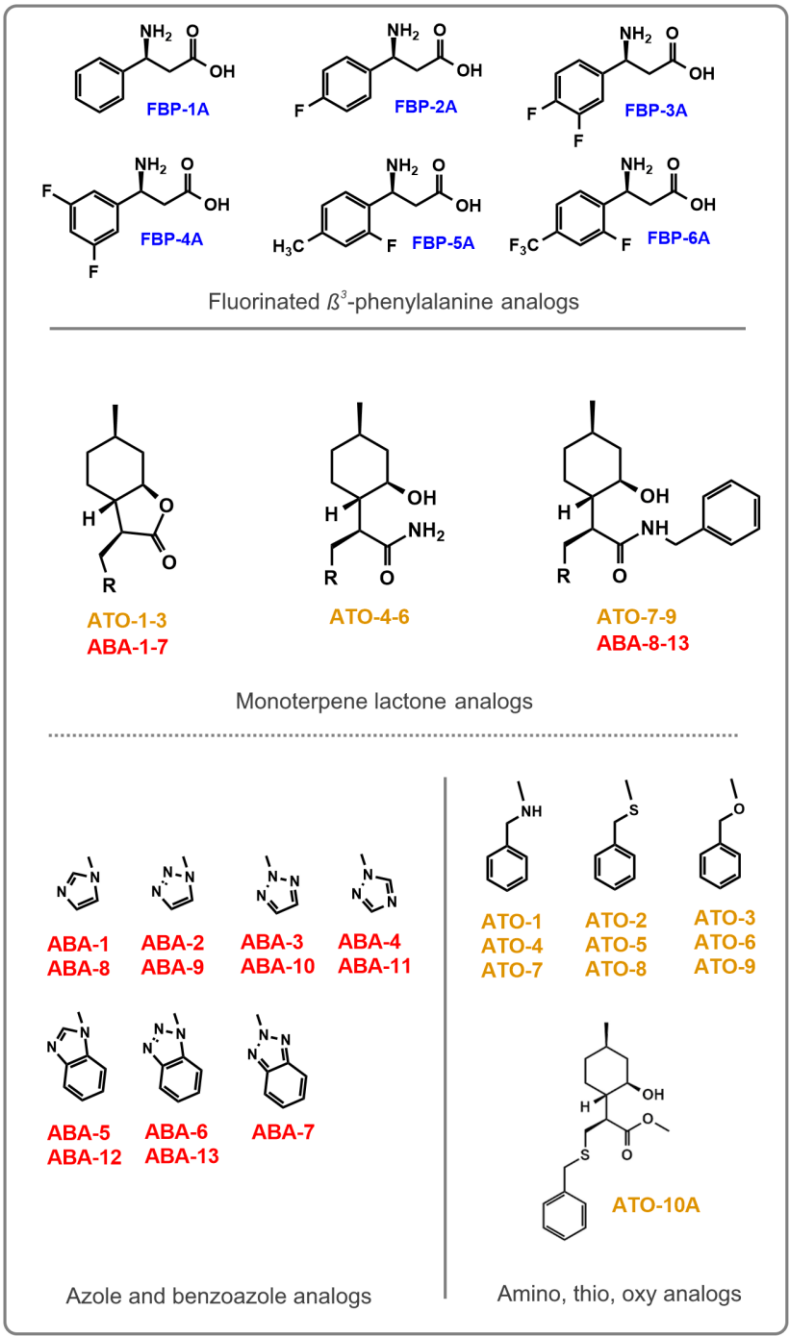

Figure 4. Structures of the analytes ("A" configurations)

5. Results and discussion

The chromatographic results reported in my thesis contribute to a better understanding of the separation mechanisms of the two applied common chiral stationary phase groups. While the leading interaction of *Cinchona* alkaloid-based CSPs is based on ion exchange, the PS-based CSPs are predominantly used for the enantioseparation of neutral compounds lacking ionizable functional groups. For this reason, the two stationary phase families cannot be characterized by the same set of compounds and, in most cases, there is also a significant difference between the mobile phases applied.

5.1. Column selection and effect of mobile phase composition

5.1.1. Effect of mobile phase composition on the enantioseparation of fluorinated β^3-phenylalanine derivatives applying ion exchanger CSPs [76]

The best performances are usually achieved for the *Cinchona* alkaloid-based CSPs in PIM when a mixture of MeOH (possessing polar and protic properties) and MeCN (as a polar but aprotic solvent) is applied most frequently. To achieve better peak shapes and promote ionic interactions, acid and base additives are needed in the mobile phase. The excess of acid is generally preferred [81]. In this way, it is always the quinuclidine group of the SO, which is protonated promoting the enantioselective ion pairing process.

The solvents of the bulk mobile phase act as *quasi*-competitors against the SO–SA complex via solvation. The protic MeOH in the solvation shell can suppress ionic and H-bonding interactions between the SO and SA, while the aprotic MeCN solvates the π-binding sites better, thus hindering the π–π while promoting the ionic interactions.

Initially, the anion exchanger-based QN–AX and QD–AX columns were studied by applying MeOH/MeCN mobile phases of different ratios (100/0, 50/50, 25/75 *v/v*) with acid (FA) and base (DEA) additives. The *Cinchona* alkaloid-based anion exchangers practically did not show significant enantiorecognition capability in the case of the studied compounds.

ZWIX(+) and **ZWIX(–)** columns were studied with varying mobile phase compositions using constant concentrations of acid (FA, 50 mM) and base (DEA, 25 mM) additives. The presented results of the ZIE columns were always obtained with these additives applied in the mobile phases in the mentioned concentrations unless otherwise stated. At first, RP conditions were tested by applying MeOH/H_2O mobile

phase systems with different compositions. Unfortunately, under all studied RP conditions, poor peak shapes and no or only small enantioselectivities were obtained.

In the following experiments, the MeOH/MeCN ratio was varied from 100/0 to 10/90 (*v/v*). As a result of the increase in MeCN content in the mobile phase (**Figure 5**), increased retention factors were obtained for all **FBP** analytes (similar to the case of anion exchangers [76]). In most cases selectivity increased up to a MeOH/MeCN composition of 25/75 (*v/v*), then it decreased slightly or leveled off. All enantioseparations were successful; however, **FBP–6** was not separated in 90% MeCN on the **ZWIX(+)** column. Resolution values developed similarly in terms of the trend. Namely, they changed according to a maximum curve on both columns, usually reaching a maximum at a composition of MeOH/MeCN 25/75 (*v/v*) on the **ZWIX(–)**, and 50/50 (*v/v*) on the **ZWIX(+)** column, as indicated in **Figure 5**.

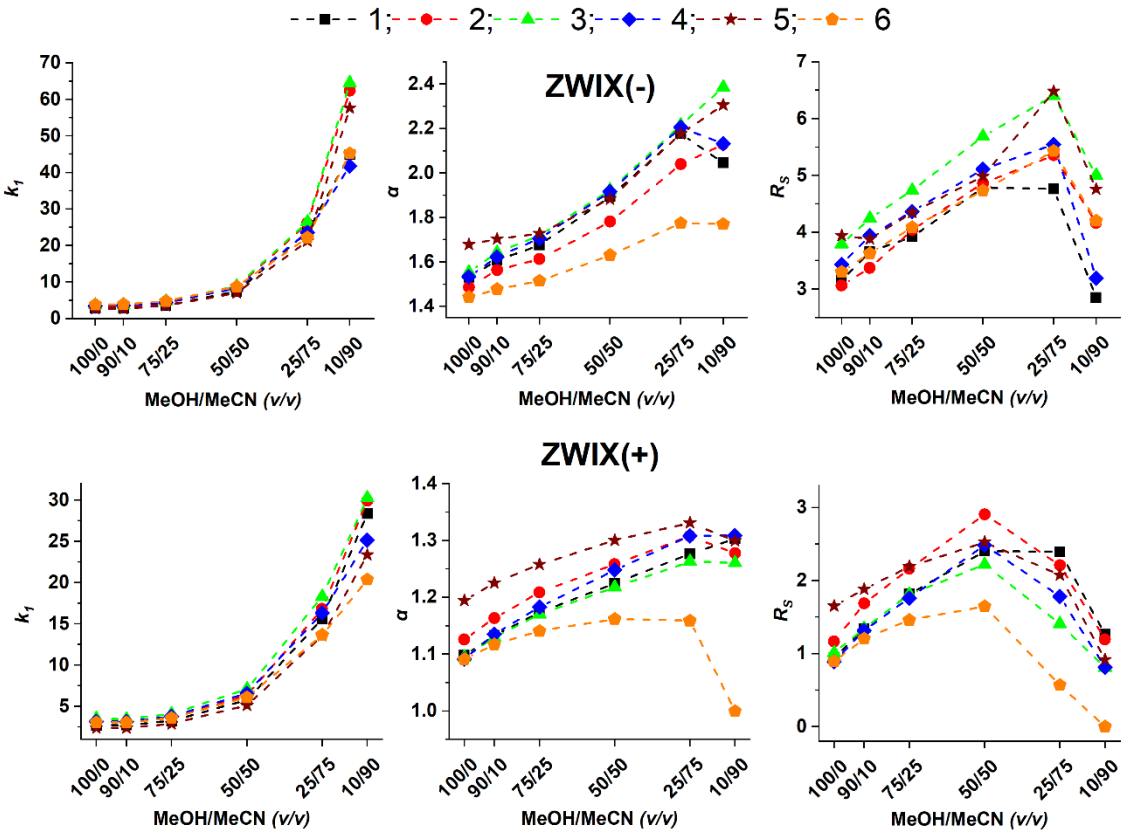

Figure 5. Effects of bulk eluent composition on the chromatographic parameters of **FBP**–analytes applying **ZWIX(–)** and **ZWIX(+)** columns

Chromatographic conditions: columns: ZWIX(–) and ZWIX(+); mobile phase, MeOH/MeCN 100/0–10/90 (*v/v*); additives, 50 mM FA + 25 mM DEA; flow rate: 0.6 mL min^{-1}; detection, 262 nm; temperature, 25 °C

These results indicate both similarities and differences between the separation mechanisms of the applied ZIE and single-ion exchanger CSPs. The increased retentions observed with higher MeCN ratios can be explained by the increased electrostatic interactions due to the decreased solvation shell of the ionized SAs and SO. In contrast, MeOH, a better solvent of SAs, can decrease the accessibility of SAs to the *Cinchona* alkaloid-based CSPs. The increase in selectivity with decreasing MeOH content suggests that H-bonding interactions play a notable role in enantioselective interactions.

5.1.2. Effect of mobile phase composition on the enantioseparations of amino, thio, and oxy analogs of monoterpene lactone derivatives applying PS-based CSPs [75]

PS-based CSPs are multimodal and often used under NP conditions with mixtures of a nonpolar hydrocarbon (most commonly *n*-hexane or *n*-heptane) and an alcohol. Alcohols with low molecular weight alcohols (e.g., EtOH, 1-PrOH, or 2-PrOH) are usually added to the bulk mobile phase as polar modifiers and the nature and concentration of the alcohol can have a deep impact on the retention and stereorecognition processes [82–84]. To reduce secondary interactions and achieve favorable peak shapes, applying acid and/or base additives may be advantageous. In POM, polar organic solvents can offer different selectivities and shorter analysis times. Generally, MeCN and short-chain alcohols, either neat solvents or binary mixtures, are used.

The effect of the nature of the alcohol was examined by applying EtOH, 1-PrOH, 1-BuOH, and 2-PrOH as polar modifiers in a constant (3.43 M) concentration in *n*-hexane (corresponding to 20 *v*% EtOH, 25.4 *v*% 1-PrOH, 31.3 *v*% 1-BuOH, and 26.2 *v*% 2-PrOH). Analyses were carried out on two pairs of structurally similar immobilized CSPs, namely Chiralpak **IA**, **IB**, and **IE**, **IC**, with all **ATO** analytes investigated. Retentions were most frequently the highest with the use of EtOH or 2-PrOH, but no general trends could be observed. **Figure 6** summarizes the number of effective separations of all ten **ATO** analytes when $R_S \geq 1.00$ was reached on the applied CSPs.

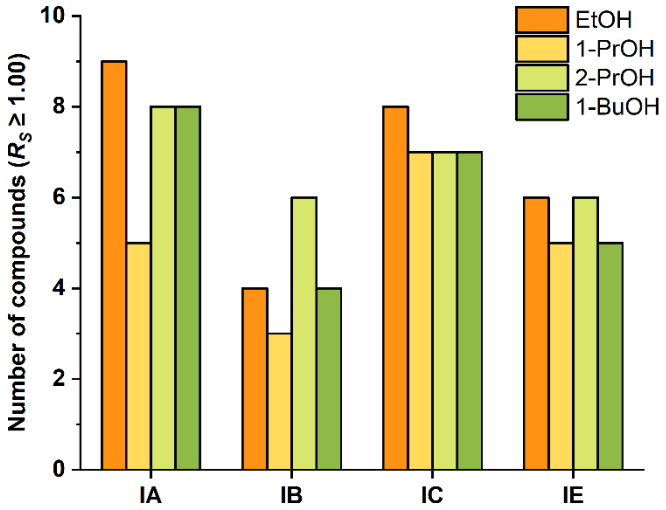

Figure 6. Effects of the nature of alcohol modifier on the resolution of **ATO** analytes in NPM applying Chiralpak PS-based columns

Chromatographic conditions: columns, Chiralpak IA, IB, IC, and IE; mobile phase, *n*-hexane/alcohol/DEA (3.43 M of alcohol in *n*-hexane, 0.1 *v*% DEA); flow rate, 1.0 mL min^{-1}; detection, 220 nm; temperature, 25 °C

The effect of alcohol concentration on the chromatographic parameters was studied first in *n*-hexane/EtOH/DEA mobile phase systems (all mobile phases contained the same amount of 0.1% (*v/v*) DEA as a basic additive.). The mobile phase consisted of EtOH in 1.30, 1.71, 3.43, and 5.14 M concentrations (which correspond to *n*-hexane/EtOH ratios of 92/8, 90/10, 80/20, and 70/30 (*v/v*), respectively). Typical NP behavior was observed for all four investigated CSPs with retentions decreasing with increasing EtOH concentrations (**Figure 7**). This effect can be explained by the better solubility of the SAs, as well as better solvation in the case of the SO, in the more polar mobile phase, along with EtOH in the solvation shells hindering H-bonding interactions, especially in the case of the most polar SAs (**ATO–4**, **5**, and **6**). The effect of 2-PrOH was also investigated in the same molar concentrations, while **ATO–1–4** and **7** analytes were selected to represent the structural differences of these SAs. The comparison of the chromatographic parameters of this investigation (**Figure A1**) with the previous one, when EtOH was applied as a polar modifier, revealed that the analytes behave essentially in a similar manner in both mobile phase systems except in some cases when EEO reversals were observed.

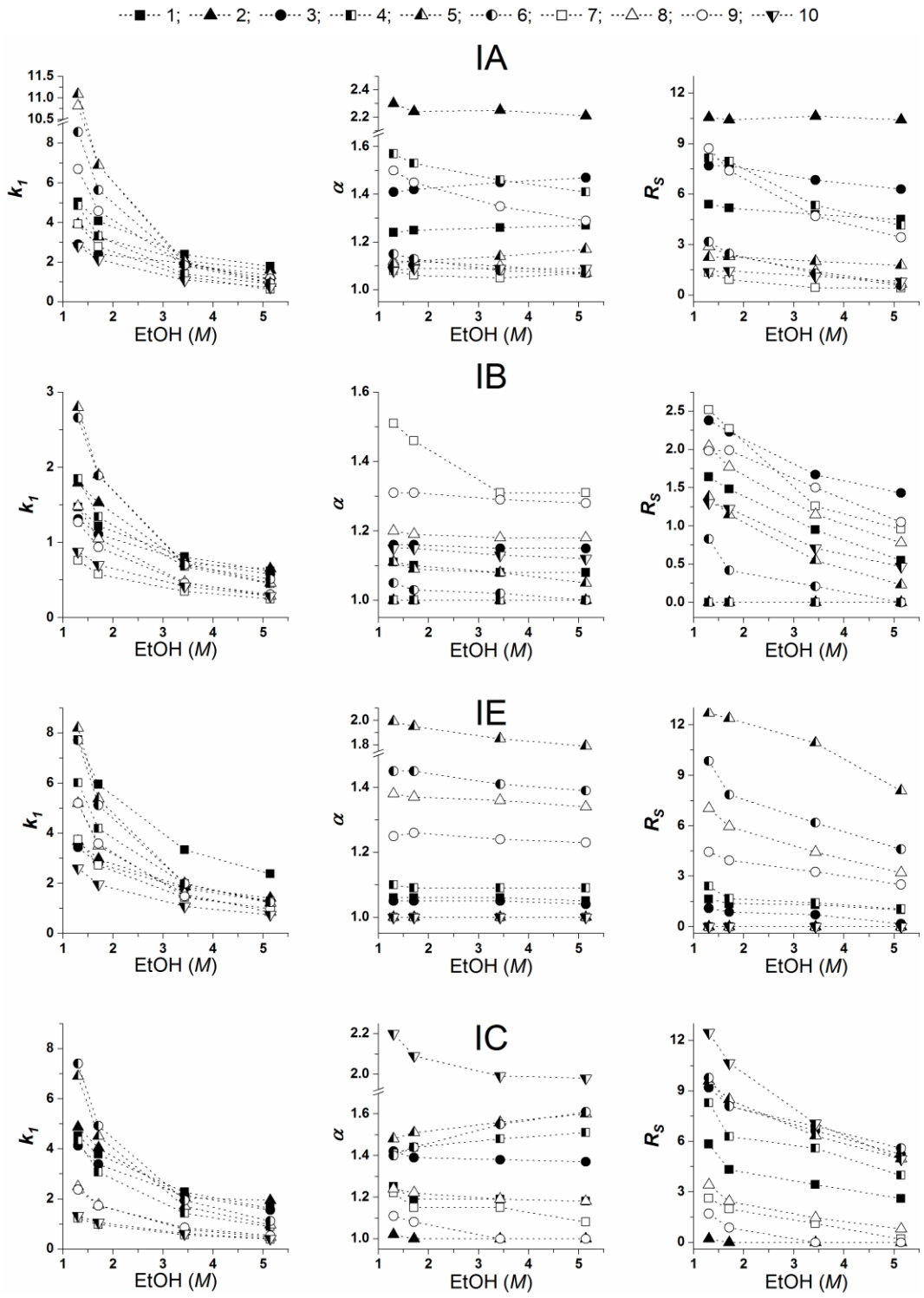

Figure 7. Effects of the concentration of the EtOH on the chromatographic parameters of all **ATO–**analytes in NPM applying **IA**, **IB**, **IE**, and **IC** columns

Chromatographic conditions: columns, Chiralpak IA, IB, IE, and IC; mobile phase, *n*-hexane/EtOH/DEA, all containing 0.1 *v*% DEA; the concentration of EtOH: 1.30, 1.71, 3.43, and 5.14 M; flow rate, 1.0 mL min^{-1}; detection, 220 nm; temperature, 25 °C

As **Figure 8** shows a few examples, the nature and concentration of the polar modifier can have significant effects on enantioseparations. EEO reversals could be

observed for five analytes (**ATO–3**, **6**, **7**, **8**, and **9**) under various chromatographic conditions, but no clear relationship between the mobile phase composition and EEO could be found.

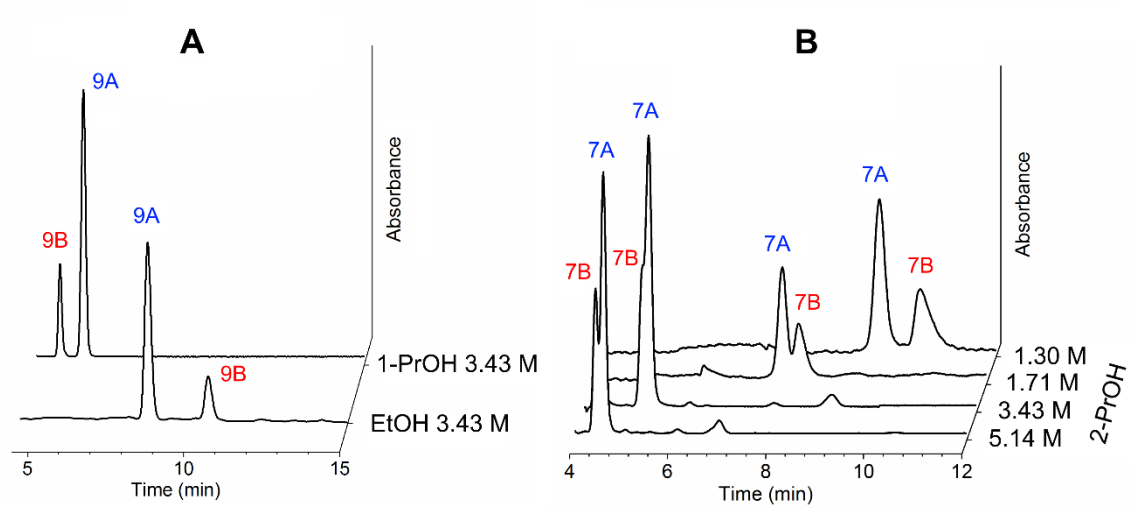

Figure 8. Representative chromatograms for the change of the EEO with the change of the nature (A) and concentration of the alcohol modifiers (B) applying **IA** column

Chromatographic conditions: column, Chiralpak IA; mobile phase, A) *n*-hexane/1-PrOH/DEA and *n*-hexane/EtOH/DEA, (3.43 M of alcohol in *n*-hexane, 0.1 *v*% DEA in all cases), B) *n*-hexane/2-PrOH/DEA (1.30 M, 1.71 M, 3.43 M, 5.14 M of 2-PrOH in *n*-hexane, 0.1 *v*% DEA in all cases); flow rate, 1.0 mL min^{-1}; detection, 220 nm; temperature, 25 °C

5.1.3. Effect of mobile phase composition on the enantioseparations of azole and benzoazole analogs of monoterpene lactone derivatives applying PS-based CSPs [74]

Initially, similar investigations were made in NP mode with all **ABA** analytes on the **cA1** column (having the same but coated-type SO as the **IA** column), where the ratio of 2-PrOH in *n*-hexane started from 20% and it increased in 20% increments until 100% without the use of the basic polar additive. Decreased retention was observed for all **ABA** analytes with increased eluent polarity. However, changes in selectivity were small and α decreased between 20/80 and 0/100 (*v*/*v*) in *n*-hexane/2-PrOH eluent composition, while R_S decreased with the increasing polarity of the mobile phase (**Figure 9**).

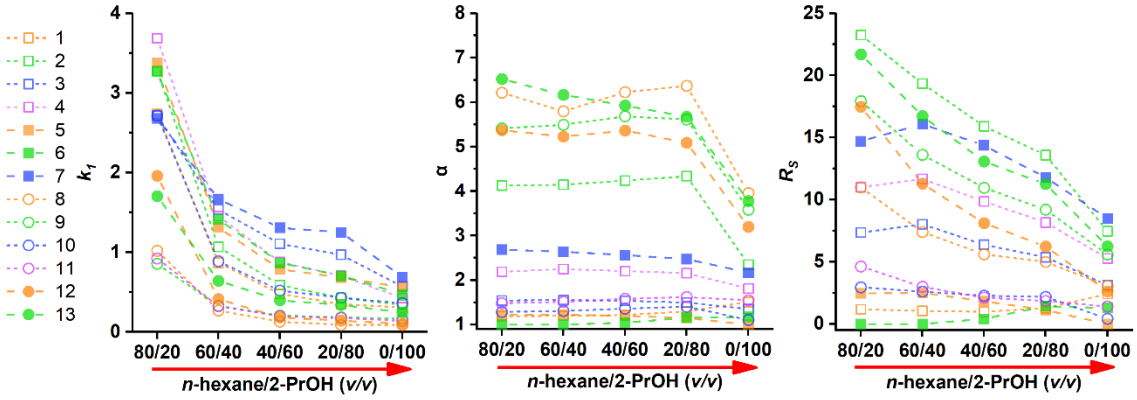

Figure 9. Effects of the eluent composition on the chromatographic parameters of **ATO–**analytes in NPM applying **cA1** column

Chromatographic conditions: column: Phenomenex Lux Amylose-1; mobile phase, *n*-hexane/2-PrOH 80/20–0/100 (*v/v*); flow rate: 1.0 mL min^{-1} (0.5 mL min^{-1} in 100% 2-PrOH); detection, 205–215 nm; temperature, 25 °C. The red arrow indicates the direction of changing the eluent composition.

A set of experiments was also carried out to compare the separation performances of covalently immobilized (**iA1**) and coated-type (**cA1**) ADMPC-based CSPs. Under NP conditions applying *n*-hexane/2-PrOH (80/20 *v/v*) eluent, twelve and eleven of thirteen SAs could be baseline resolved using coated and immobilized ADMPC selectors, respectively. (**Table A1** shows examples for the enantioseparation of a few **ABA** analytes). In most cases, retention factors of the first peaks were lower, while enantioselectivities and resolutions were higher on the coated-type column. *Thunberg et al*. reported similar results, suggesting that the higher degree of achiral interactions led to longer retentions and lower enantioselectivities on the immobilized phase [85]. The reason could lie in the structural alterations observed during immobilization, as the possible effects of the synthesis of the immobilized-type CSPs were summarized by *Shen et al*. [86]

Experiments were made to compare the differences between the coated- and immobilized-type CSPs in POM as well. A reduced set of analytes (**ABA–5**, **6**, **8**, and **9**, representing the structural differences of these analytes) was injected into the same five neat PO mobile phases. Higher differences can be seen, depending on the nature of the PO solvents, than in NPM, e.g., drastic performance differences in MeCN or EEO reversal of **ABA–5** in MeOH (**Table 1**; for data of other PO mobile phases, see **Table A2**). In most cases, enantioselectivities and resolutions were slightly higher on the coated-type column. However, retentions strongly depended on the PO mobile phase. For example, in MeCN, MeOH, and EtOH higher, while in 1-PrOH, and 2-PrOH lower retentions were observed on the coated-type column, suggesting a more complex

influence on the retention mechanism due to the different solvation shells associated with each column type.

In PO mode, five different neat solvents, MeCN, MeOH, EtOH, 1-PrOH, and 2-PrOH were used. The best results were obtained with MeCN and EtOH as solvents both offering twelve enantioseparations with $R_S \geq 1.5$ of thirteen analytes. In most cases, retention factors (k_1), applying only neat alcohols, decreased in the order EtOH > MeOH > 1-PrOH > 2-PrOH in harmony with their polarity, except for EtOH.

Table 1. Effects of selector immobilization on the chromatographic parameters in the enantioseparation of azole analogs of monoterpene lactones and amides in POM applying coated (**cA1**) and immobilized (**iA1**) ADMPC-based CSPs.

Analyte	k_1, α, R_S	Mobile phase and column type			
		MeCN		MeOH	
		cA1	iA1	cA1	iA1
5	k_1	1.04	0.16	1.16	0.51
	α	3.02	1.00	1.17	1.35
	R_S	6.76	0.00	1.13	2.08
	EEO	A < B	-	B < A	A < B
6	k_1	0.53	0.29	1.40	0.69
	α	1.14	1.00	1.06	1.38
	R_S	0.55	0.00	0.84	2.80
	EEO	A < B	-	B < A	B < A
8	k_1	3.30	0.01	0.13	0.05
	α	1.80	1.00	2.39	3.24
	R_S	2.36	0.00	0.97	1.07
	EEO	B < A	-	B < A	B < A
9	k_1	2.16	0.86	0.26	0.09
	α	1.56	1.69	4.99	2.93
	R_S	2.35	2.82	2.50	2.87
	EEO	B < A	B < A	B < A	B < A

Chromatographic conditions: columns, Phenomenex Lux Amylose-1 (coated, **cA1**) and i-Amylose-1 (immobilized, **iA1**); mobile phase, 100% MeCN, and 100% MeOH; flow rate, 1.0 mL min^{-1}; detection, 215 nm; temperature, 25 °C

In a similar set of experiments, the performance of the **cC1** column was compared to that of the **cA1** column. In this case, markedly reduced enantiorecognition ability was obtained with the cellulose-based CSP, and none of the studied analytes could be baseline-separated in any of the five polar organic solvents. Based on these results, it can be concluded that the amylose-based CSP offers a much better fit for the studied analytes than the cellulose-based one, independently of the applied chromatography mode.

5.2. Effect of the nature and concentration of mobile phase additives

5.2.1. Effect of mobile phase additives on the enantioseparation of fluorinated β³-phenylalanine derivatives applying ion exchange-based CSPs [76]

In addition to the eluent composition discussed above, both the quality and the amount of acid and base added to the mobile phase may significantly influence chromatographic properties. *Cinchona* alkaloid-based ZIE CSPs work best when the acid and base are present in the mobile phase in a 2:1 ratio [81].

Previous investigations showed that the nature of the acid had no marked effect on the chromatographic parameters when using the same base [87]. As a consequence, for these experiments, FA was applied as the acid component (50 mM), and organic amines EA, DEA, and TEA (25 mM) were used as bases in two different eluent systems (MeOH/MeCN 50/50 and 100/0 (*v/v*)) on the **ZWIX(–)** column. In pure MeOH, k_1 values differed slightly but to a greater extent in MeOH/MeCN 50/50 (*v/v*) (**Figure 10**), while the elution strength was TEA < DEA< EA in all cases. The changes in α and R_S, in turn, were much less marked. The basicity of the amines is rather similar (EA, DEA, and TEA have pK_a values of 10.70, 10.84, and 10.75, respectively [88]). Thus, it can be stated that the number of ethyl substituents of the amine can significantly affect the retentive properties through the size and shape of the alkyl amine ions, furthermore, this property depends strongly on the eluent composition.

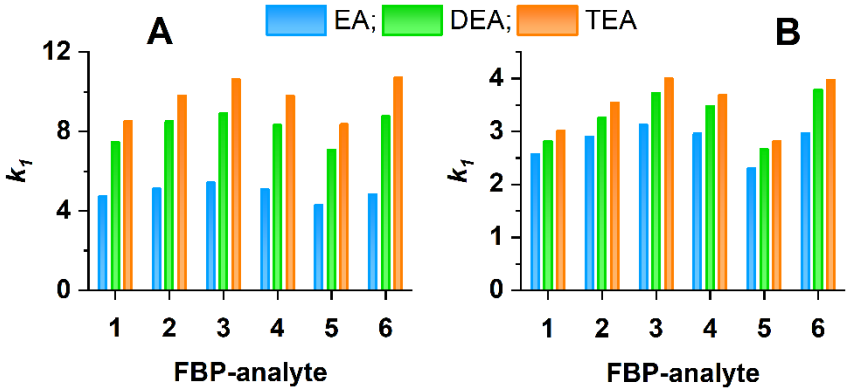

Figure 10. Effects of the nature of the base additive on the retention factor of the first-eluting enantiomer (k_1) of **FBP**–analytes applying **ZWIX(–)** column

Chromatographic conditions: column: ZWIX(–); mobile phases, **A)** MeOH/MeCN 50/50 (*v/v*), **B)** MeOH/MeCN 100/0 (*v/v*); additives, 50 mM FA + 25 mM EA/DEA/TEA; flow rate: 0.6 mL min^{-1}; detection, 262 nm; temperature, 25 °C

For the quantitative description of the chromatographic ion exchange process, the simple stoichiometric displacement model is applied in most cases (**Eq. (7)**) [89,90].

$$\log k = \log K_Z - Z \log[X] \quad (7)$$

The model assumes a linear relationship between the logarithm of the retention factor and the logarithm of counterion concentration (X), where the plot of log k vs. log [X] provides the slope. This is related to the effective charge Z (ratio of the charge number of the SA and the counterion), whereas the intercept is related to the ion exchange equilibrium constant K_Z. To gain a deeper insight into the details of the retention mechanism, the acid-to-base molar ratio was kept constant at two, with varying concentrations of both the acid (FA, 12.5–200 mM) and the base (DEA, 6.25–100 mM) in 100% MeOH applying both **ZWIX(+)** and **ZWIX(–)** columns. As **Figure 11** shows, linear fittings could be achieved with $R^2 > 0.97$ in all cases, supporting the validity of the model in the studied systems.

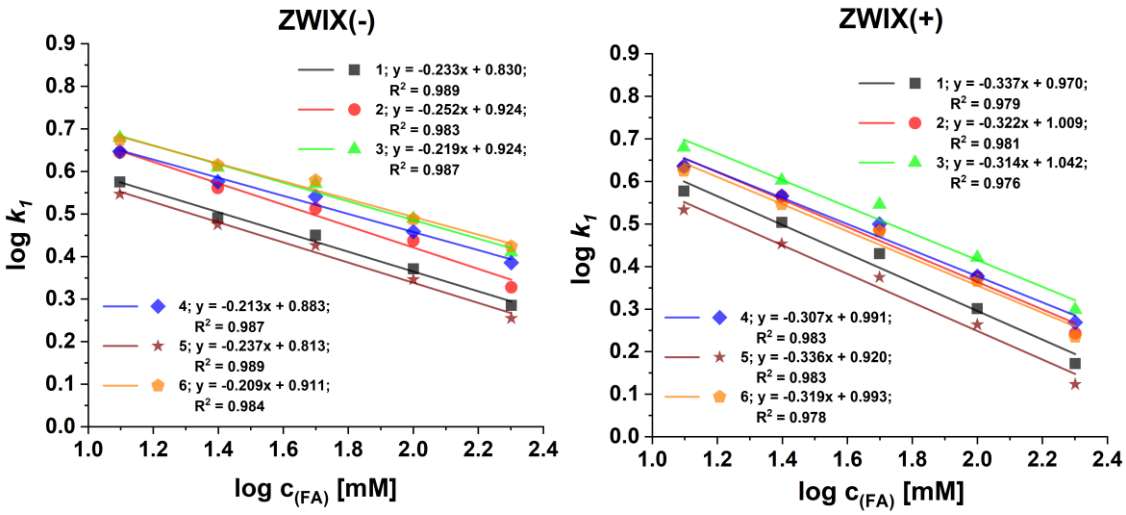

Figure 11. Effects of counterion concentration on the retention factor of the first-eluting enantiomer (k_1) of **FBP** analytes applying **ZWIX(–)** and **ZWIX(+)** columns

Chromatographic conditions: columns, ZWIX(–) and ZWIX(+); mobile phase, MeOH containing DEA/FA (mM/mM), 6.25/12.5, 12.5/25, 25/50, 50/100, and 100/200; flow rate, 0.6 mL min^{-1}; detection, 262 nm; temperature, 25 °C

The slopes of the log k vs. log [X] plots varied in a narrow range, between 0.21 and 0.25 for the **ZWIX(–)**, and between 0.31 and 0.34 for the **ZWIX(+)** column. These are in accordance with earlier results obtained with zwitterionic CSPs applied in zwitterionic mode [28,79,91]. Reduced retentions are obtained with increasing counterion concentration as it can be seen in **Table A3**, which shows examples for a few of the **FBP**

analytes. At the same time, however, enantioselectivity remained nearly unchanged, highlighting an advantageous property of the studied ZIE CSPs. That is, the retention can be tuned by varying the concentration of the counterions without having a significant loss of enantioselectivity.

5.2.2. Effect of mobile phase additives on the enantioseparation of amino, thio, and oxy analogs of monoterpene lactone derivatives applying PS-based CSPs [75]

Enantioseparations (including EEO reversal) on PS-based CSPs can be influenced in different ways [34–36]. Besides changing the ratio of polar modifiers (as discussed before), applying mobile phase additive(s) is another possibility to fine-tune chromatographic separation.

Investigation of the effect of the nature of basic additive on **ATO** analogs, separations were carried out by injecting **ATO–1–4** and **7** onto the **IA** column as it has the most widely used ADMPC SO among the polysaccharide-based CSPs. The mobile phase consisted of *n*-hexane/EtOH/base 80/20/0.1 (*v/v/v*). The selected bases were EA, DEA, TEA, and triethanolamine (TEOA). They exerted only a slight effect on chromatographic parameters, k_1, α, *and* R_S, indicating that the bases participate in the separation process in a similar manner. Their competition for the binding sites of the stationary phase and contribution to the reduction of band broadening was practically independent of their nature for the studied chromatographic systems.

5.2.3. Effect of mobile phase additives on the enantioseparation of azole and benzoazole analogs of monoterpene lactone derivatives applying PS-based CSPs [74]

Investigations were carried out by measuring all **ABA** analytes. In NPM, applying *n*-hexane/2-PrOH/additive 80/20/0.1 (*v/v/v*) was applied as eluents with FA and DEA used as additives, either separately or together. To investigate the possible effects of additives in the PO mode, measurements were carried out using neat EtOH or MeCN as the eluent. In HPLC experiments, additives are most frequently added to the bulk eluent in volume percentage. Comparing the results might be difficult in these cases since the molar concentrations will differ. To make the results easier to compare in this series of experiments, 1:1 and 2:1 molar ratios of FA and DEA were applied. (The molar concentration of DEA was set at 9.71 mM, which corresponds to 0.1 *v*%, while the 2:1 molar ratio of FA and DEA approximately corresponds to 0.1/0.1 *v/v*%.).

Based on results discussed by *He* [92,93] and *Mskhiladze* [93] additives were expected to affect chiral recognition more markedly in PO than in NP mode. Comparing the data obtained in NPM, EtOH, and MeCN (see examples of **ABA–1**, **8**, and **12** in POM in **Table A4**), the additives showed only a slight effect on the chromatographic parameters, with the exception, when adding only FA. In the cases of the structurally strongly related **ABA–1** and **8** (having the highest pK_a values, calculated with the Marvin Sketch v. 22.16 software, ChemAxon, Budapest) resulted in poor peak shapes and drastically reduced resolutions in all three eluents. Their enantioseparation was even unsuccessful in NPM. However, their retention slightly increased compared to the other cases where no additives, only DEA, or DEA and FA together were used. In the presence of FA, the formation of ion pairs from the protonated base and the formate ion can be a plausible explanation for the higher retention and diminished enantiorecognition. The formation of protonated ions instead of ion pairs can be expected in POM, which can be responsible for the reduced retention and poor peak shape, although the influence of other structure-related effects cannot be excluded. The application of additives did not cause a change in EEO in the studies presented in Section 5.2.

5.3. Structure-retention relationships

As mentioned earlier, one of the major objectives of this thesis work was to explore the effects of changes in structural properties and to interpret the effect of the structure on chiral recognition by using compounds with significant structural analogy. Thus, utilizing comparative chromatographic examinations, the effects of the different molecular structures on the chiral separations and chromatographic parameters have been studied by exploring SO–SA interactions.

5.3.1. SO–SA interactions between the zwitterionic CSPs and the fluorinated β^3-phenylalanine derivatives [76]

Earlier studies were carried out with the use of **FBP–1** and **2** besides various other analogous. A study compared several β^3-AA derivatives [79] applying ZIE CSPs, but only one of twenty-three analytes was fluorinated. In another study [78] the enantiomers of eighteen β^3-AA derivatives were separated applying macrocyclic glycopeptide-based CSPs. Eight of the analytes were halogenated, two of them fluorinated. The presence of different halogen substituents (F, Cl, Br) at identical positions did not lead to significant

change in chiral recognition; however, a minor change in resolution was observed. Notably, baseline separations for these analytes were not attained.

When ZIE CSPs were applied in my work in order to investigate the effect of the position of the fluorine atoms, it could be stated that all SAs, both the fluorinated and the non-fluorinated **FBP–1**, behaved in a rather uniform way, that is, no vital differences in the chromatographic properties could be observed (**Figure 5**). Slight differences in retention and enantiorecognition are expressed in some cases, e.g., when comparing the chromatographic properties of *para*-substituted analyte **FBP–2** to the non-fluorinated one. Here, retentions were lower for the latter, while no significant difference in enantioselectivities could be detected. In the case of **FBP–2–4**, lesser differences were observable. This observation suggests that the main interactions responsible for retention and enantiorecognition were not radically modified by the structural changes related to the fluoro-substitution of these SAs. **FBP–5** eluted with the lowest retention. Interestingly, these lowest retentions were accompanied by the highest enantioselectivities in most of the cases, suggesting that methyl substitution together with the fluorination of the aromatic ring results in such a favorable structure, where the non-selective interactions formed between the SA and SO can markedly be decreased. In the case of **FBP–6**, exchanging all H atoms of the methyl group for F atoms resulted in higher k, but lower α values in comparison to those of **FBP–5**. Furthermore, the lowest α values were obtained in the case of **FBP–6** on both columns, suggesting that the structural changes can affect the enantiorecognition markedly without strongly affecting retention.

EEOs were determined in all cases, and they were $R < S$ for all **FBP** analytes in all cases on the **ZWIX(–)** column, and $S < R$ on the **ZWIX(+)** column without any exception, illustrating well the pseudoenantiomeric properties of the applied columns that allow for an easy reversal of elution orders by column switching.

5.3.2. SO–SA interactions between PS-based selectors and the amino, thio, and oxy analogs of monoterpene lactone derivatives [75]

All **ATO** analytes were analyzed by chromatography with all studied Chiralpak columns applying the same *n*-hexane/EtOH/DEA 80/20/0.1 (*v/v/v*) mobile phase. Based on the separation characteristics and the wide variety of SOs and SAs, numerous comparisons can be made about relationships between the structure of SOs and SAs. Since both **IA** and **IB**, and **IE** and **IC** pairs have the same phenylcarbamate modifier

groups, the separation mechanisms on amylose- and cellulose-based SOs are comparable. Retentions were higher on amylose-based SOs, indicating that the analytes had stronger non-selective interactions in the cavities of the helical amylose chain, except **ATO–2** and **3**, where k_1 was higher on **IC** rather than **IE**. On the other hand, no direct correlation between enantiorecognition and CSP structure could be found, as selectivity and resolution were variably larger or smaller when comparing results between differently modified PS-based CSPs. The same can be said about EEOs, except that all amides (**ATO–4–6)** eluted with the same EEO on the cellulose-based **IE** and **IC**. Similar observations were made when comparing CSPs with different phenylcarbamate modifiers attached on the same PS chains, as chlorination usually caused higher retentions and the enantiorecognition and EEOs varied, even if the results obtained from **IG** were also considered. A variety of examples for EEO differences caused by the change of the SOs are shown on **Figure 12**, when either the PS type or the phenylcarbamate groups have been changed.

The effects of the position of methyl and chloro substituents on the phenyl moiety (**IF** *vs* **IG**) can also be analyzed. In most cases, higher k_1, α, and R_S were registered on **IG** than on **IF** providing evidence for the significant role played by steric effects of the substituents of the phenylcarbamate moiety on chiral recognition. It is interesting to note that **ID** (possessing 3-chlorophenylcarbamate moieties) exhibited the lowest chiral recognition ability (**ATO–4** is an exception). Chromatographic parameters were usually higher for **ATO–5** than for **10**, which is probably due to the stronger H-bonding interactions with the SO by the amide group of **ATO–5**.

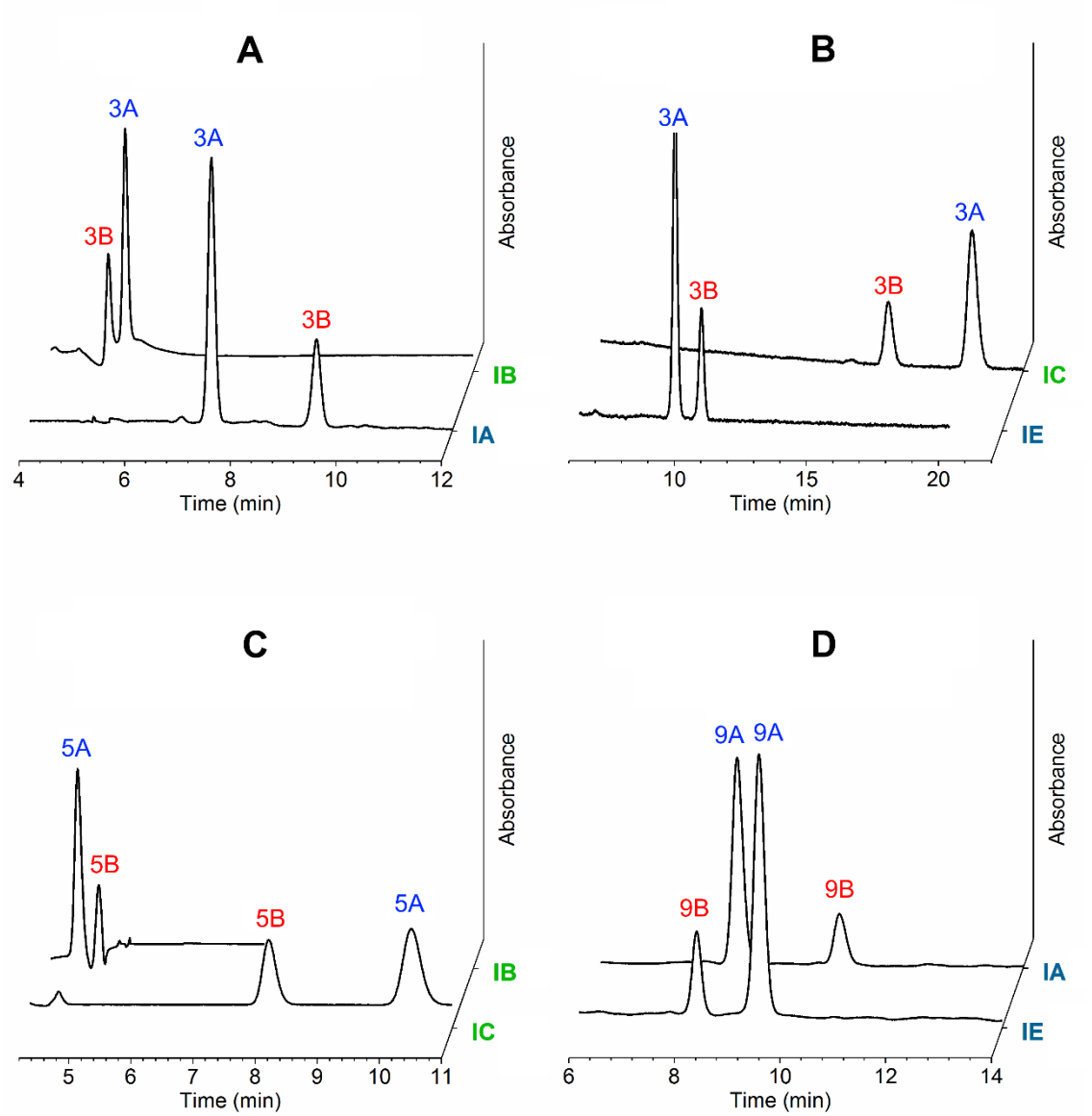

Figure 12. Representative chromatograms for the change of the EEO with the change of different PS-based CSPs and mobile phases.

Chromatographic conditions: columns, Chiralpak IA, IB, IC, IE; mobile phase, A) and D) *n*-hexane/EtOH/DEA, B) *n*-hexane/2-PrOH/DEA, C) *n*-hexane/1-PrOH/DEA (3.43 M of alcohol in *n*-hexane, 0.1 *v*% DEA in all cases); flow rate, 1.0 mL min^{-1}; detection, 220 nm; temperature, 25 °C

ATO analytes can be grouped by their structures (**Figure 4**) as **ATO–1–3**, **4–6**, and **7–9** being lactones, amides, and *N*-benzylamines, respectively, with each group having benzylamino, benzylsulfanyl, and benzyloxy functional groups. **ATO–10** has a methyl ester group instead of the amide in **ATO–5**. Results organized by the calculated polarity (log P) and volume [$Å^3$] of the molecules are collected in **Table** A5. All data were calculated with the Marvin Sketch v. 17.29 software (ChemAxon, Budapest) allowing to conclude that retention usually decreased slightly with increasing analyte polarity. However, lactones behave differently, which is probably due to different

interactions made by the lactone ring. The ring-opened lactones have larger volumes, even larger when the extra benzyl group is attached to the molecules. This increase in size is in correlation with the decrease in retention. This finding suggests that a molecule with a smaller size fits better into the chiral cavities of the PS chains and, therefore, SO–SA interactions are enhanced.

5.3.3. SO–SA interactions between PS-based selectors and the azole and benzoazole analogs of monoterpene lactone derivatives [74]

During NPM investigations, the applied **cA1** selector showed unexpectedly high enantioselectivities, even when neat 2-PrOH was applied (baseline separations could be achieved for nine analytes of thirteen). Regardless of the mobile phase composition, amides were less retained than lactones, suggesting that the lactone unit significantly contributed to retention. However, interactions formed in the presence of the lactone unit were mostly non-selective, rarely leading to higher enantioselectivities. In similar mobile phase systems, the alcohol modifier was found to be incorporated into the structurally same ADMPC CSP [94,95]. The displacement of *n*-hexane by the polar modifier led to remarkable alterations in the steric environment of the chiral cavities of the ADMPC selectors. POM separations resulted in less uniform chromatographic parameters as described in Section 5.1.3. However, selectivities of most of the compounds changed in accordance with the polarity of the POM eluents. Enantioselectivity of five of the seven lactones increased with the polarity of the eluent, while four of the six amides showed the opposite effect. It is interesting to note that these four amides (**ABA–8, 9, 12,** and **13**) had formed a group in NPM with exceptionally high enantioselectivities (along with lactone **ABA–2** with the same functional group as in **ABA–9**). All these compounds have the *N*-azole and *N*-benzoazole bond in the same position, whereas N atoms are in 1,3 and 1,2,3 positions. This position of the N atoms and related bonds probably greatly contributed to the formation of enantioselective interactions between the SO and SAs. It is presumable, that the polarity of solvents also affects this effect to an extent. 2-PrOH and MeCN had different effects on separation. Interestingly, extreme differences were observed between the chromatographic parameters when using neat 2-PrOH or 1-PrOH. For example, the selectivity of **ABA–9** was 3.27 in 2-PrOH and 44.85 in 1-PrOH (**Figure 13**), and different EEOs were recorded in the case of **ABA–1, 3, 5**, and **6**.

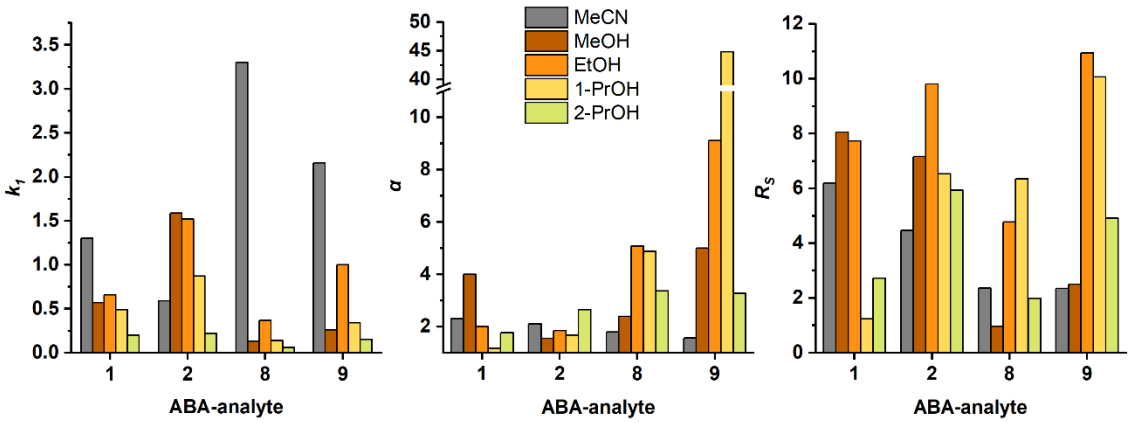

Figure 13. Effects of neat polar organic eluents on the chromatographic parameters of **ABA–1**, **2**, **8**, and **9** analytes in POM applying **cA1** column

Chromatographic conditions: column, Phenomenex Lux Amylose-1; mobile phases, MeCN, MeOH, EtOH, 1-PrOH, 2-PrOH; flow rate, 1.0 mL min^{-1} (0.5 mL min^{-1} in 1-PrOH and 2-PrOH); detection, 215 nm; temperature, 25 °C

These findings suggest that the nature of alcohol affects the interactions formed between the selector and the analyte not only through its polarity. Generally, the nature of the polar solvent affects retention and enantiorecognition in several ways, resulting in pronounced differences, even in the case of structurally related compounds. These findings suggest the necessity of further investigation of the retention mechanisms in POM.

5.4. Hysteresis phenomena of the polysaccharide-type CSPs [74]

The utilization of mobile phases based on binary solvent systems is the most frequently applied approach for fine-tuning retention and selectivity in liquid chromatography. Typically, when changing the composition, it is not expected that, in the case of a given composition, retention and selectivity depend on the direction from which the given composition is approached. However, this seems to be the case for PS-based selectors under certain chromatographic conditions.

Hysteretic (a.k.a. history-dependent) behavior based on the eluent composition of PS-based CSPs was first discovered and examined with scientific rigor by *Németh et al.* [44], and later further studies were made by them [45–47]. Since the phenomenon is thought to be associated with the higher-order structure of the PS chains, the immobilization way of the PS SOs is expected to influence the hysteresis, as it was reported for a few compounds [44].

Precision and accuracy play a vital role in analytical measurements. However, in this thesis, the difference in results (a.k.a. the extent and direction of changes) between the measurement series is the most important to be able to describe findings, whereas the extent of errors is one of the most important aspects, when investigating the hysteresis phenomena. In such instances, complete hysteresis cycles were repeated to ensure accuracy. Relative standard deviations (RSD%s) were calculated from three parallel consecutive measurements of three different analytes in three different mobile phase compositions for each set of sample analytes. **Table A9** shows these RSD% values on the example of azole analogs.

5.4.1. Importance of column treatment

Previously, all PS-based CSPs applied in this study were used only in NP conditions, including the shipment from the manufacturer and column storing (both in *n*-hexane/2-PrOH 90/10 (*v/v*) without additives). The instruction manuals of the columns state that changing the chromatographic mode is possible, but changes in R_S and t_R may be observed, and switching back to NPM from POM is not recommended [96,97].

Németh et al. extensively tested the effects of mode switchings, and recommended column washing protocols as well [44,46]. Based on their recommendations, the following washing procedures were applied when switching the chromatographic modes, to properly reset the CSPs to their "original" state:

- From NPM **to POM**: 10 V_0 2-PrOH as transition eluent, then
  10 V_0 **2-PrOH/EtOH 50/50** (*v/v*), then equilibrate with the mobile phase
- From POM **to NPM**: 10 V_0 2-PrOH as transition eluent, then
  10 V_0 ***n*-hexane/EtOH 90/10** (*v/v*), then equilibrate with the mobile phase
- In POM: neat solvents also "reset" the column to its "original" state. However, the appropriate switching eluent was also used before the start of every new measurement series (either in NPM or POM) to provide the same conditions in all cases.

The importance of proper mode switching is illustrated with the example of **ABA–5** in **Figure 14.**

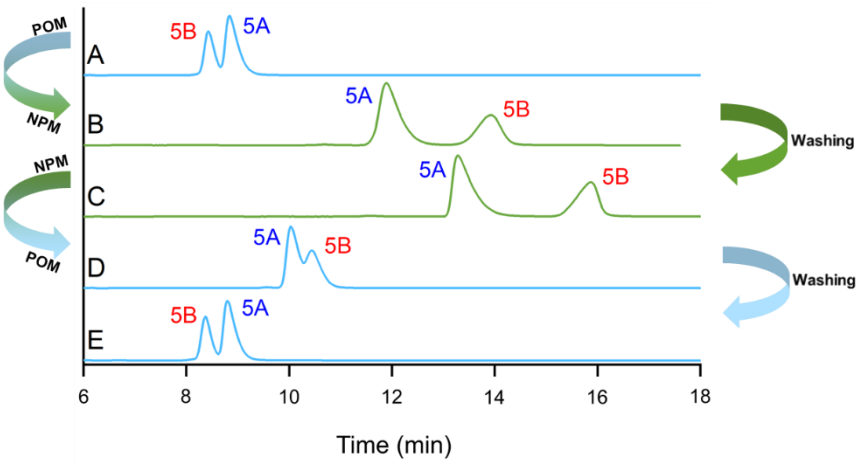

Figure 14. Effects of mode switching and applying washing protocols described above on the chromatograms of **ABA–5** applying **cA1** column

Chromatograms are in order in time from top to bottom, and colors represent the same eluent composition. Arrows on the left side indicate mode switches, while arrows on the right side indicate the differences between before and after states when using the washing protocols.

Chromatographic conditions: column, Phenomenex Lux Amylose-1; mobile phase, **A)**, **D)**, and **E)** 2-PrOH, **B)** and **C)** *n*-hexane/2-PrOH 80/20 (*v/v*); flow rate, 1.0 mL min^{-1} in *n*-hexane/2-PrOH 80/20 (*v/v*), 0.5 mL min^{-1} in 2-PrOH; detection, 215 nm; temperature, 25 °C

This means that results of NPM measurements applying a high ratio of polar modifier (e.g. **Figure 9**) only can be interpreted if the direction of solvent ratio changing is given (which is usually increasing the polar modifier ratio) and an appropriate washing protocol is applied after, or before the next measurement series, especially in the case of coated-type PS CSPs.

5.4.2. Chromatographic environment during the investigations of the hysteresis phenomenon

Application of the **cA1** column in NPM, *n*-hexane/2-PrOH, in PO mode 2-PrOH/1-PrOH, 2-PrOH/MeOH, MeOH/MeCN, and MeOH/EtOH mobile phase systems was investigated to gather more data about the unique hysteretic properties of the amylose-based CSP. Chromatographic parameters with mobile phase compositions of 100/0, 80/20, 60/40, 40/60, 20/80, and 0/100 (*v/v*) were measured to create hysteresis loops. The previously described washing protocol was applied before each series of hysteresis loop measurements, while within one hysteresis loop measurement, only equilibration with the actual mobile phase was performed. The **iA1** column was also utilized in POM with 2-PrOH/MeOH eluents to gather information about the possible effects of selector immobilization. To evaluate the impact of the cellulose backbone on

the hysteretic behavior, a cellulose-based column with the same DMP selector would be the best choice. Unfortunately, **cC1** in POM was inefficient in the enantioseparation of the studied analytes. Consequently, **cC4**, another cellulose-based column was employed for this purpose. (Unfortunately, there is no Lux Amylose column available with the same *tris*-(4-chloro-3-methylphenylcarbamate) selector, so the results obtained are compared to the results collected with the ADMPC-based **cA1** column.). 2-PrOH/MeOH and MeOH/MeCN systems on the **cA1** column were investigated with all thirteen **ABA** analytes, while a reduced set (three to five) of **ABA** analytes was selected for investigating other compositions and columns.

5.4.3. Evaluating the obtained data of hysteresis

To illustrate the phenomenon of hysteresis, a hysteresis curve, instead of chromatograms, is generally applied, where k_1, k_2, or α is plotted against the solvent composition. The hysteresis curve is a good solution for visualization of the changes, but it has some severe limitations. On the one hand, it does not provide information for the single enantiomers about the accurate extent and direction of the changes. On the other hand, it does not allow direct comparison of the results obtained in different systems. For the quantitative description of the phenomenon, hystereticity (in analogy to selectivity) was introduced very recently by *Horváth et al*. [47]. Hystereticity factor (v) was defined as the ratio of the two retention factors determined for the same enantiomer under the same conditions but with two different antecedents, where the larger value is the numerator, and the smaller is the denominator. The hysteretic behavior causes changes in retention times independently for each enantiomer. Since both the degree and the direction of the change in retention time can be different, enantioselectivity may stay constant or hysteresis of the enantioselectivity also happens. Moreover, EEO reversals can also take place during the hysteresis which could lead to erratic interpretations. To illustrate all possible consequences of the phenomenon, an example is shown in **Figure 15**. Applying the **cA1** column with a 2-PrOH/1-PrOH mobile phase system, the hysteretic behavior resulted not only in remarkable changes in enantioselectivity but also reversed EEO in the case of **ABA–3**.

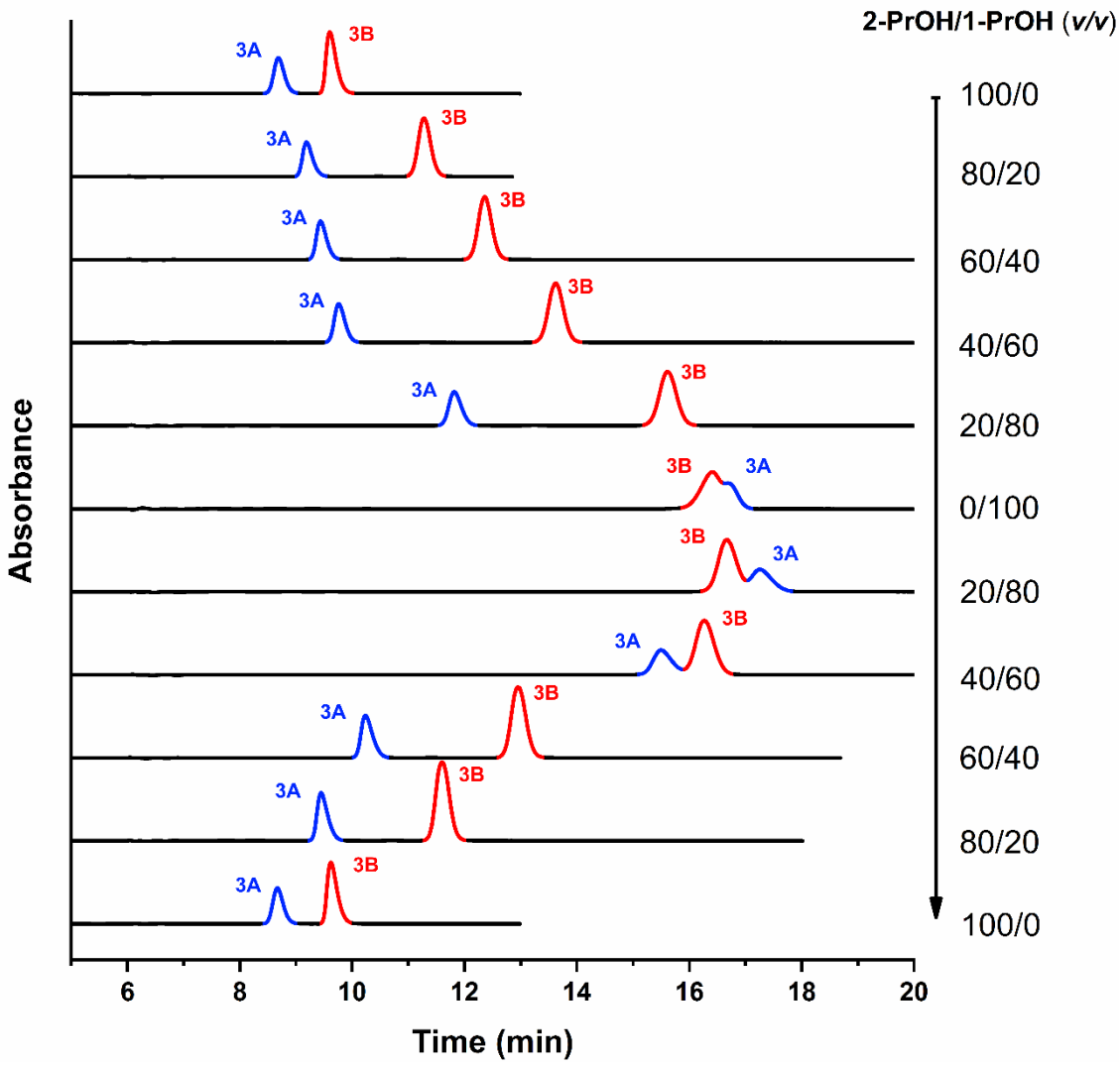

Figure 15. Chromatographic representation of the hysteretic behavior of the **cA1** CSP observed with **ABA–3**.

Chromatographic conditions: column, Phenomenex Lux Amylose-1; mobile phase, 2-PrOH/1-PrOH 100/0–0/100 (*v/v*); flow rate, 0.5 mL min^{-1}; detection, 215 nm; temperature, 25 °C

To overcome the erroneous results caused by the classical way of calculating separation factors, a slightly modified definition is presented: instead of elution order, the hystereticity factor is defined on the basis of the direction from which the given composition is approached (**Eqs. (8) and (9)**):

$$\upsilon_A = k_{A_b}/k_{A_f} \tag{8}$$

and

$$\upsilon_B = k_{B_b}/k_{B_f} \tag{9}$$

where k_{Af} is the retention factor of enantiomer "A" measured at a certain mobile phase composition from the forward direction (100/0), while k_{Ab} is the retention factor of

the same enantiomer "A" measured at the same mobile phase composition from the backward (opposite) direction (from 0/100). Analogously, v_B can be defined for enantiomer B (**Eq. (9)**). Applying this approach, information on how each enantiomer is affected can be extracted: the higher the deviation of hystereticity from one, the stronger the hysteretic effect is.

For a more accurate evaluation of whether the deviation of hystereticity from one is significant, statistical evaluation is needed. RSD%s were calculated from three parallel consecutive measurements of three different analytes in three different mobile phase compositions (**Table A9**). Confidence intervals of 95% probability were calculated, while also taking the propagation of error into account. The highest value of the RSD% (0.8%) was used for all further calculations. A confidence interval of 1 ± 0.028 was applied for all presented values. To help evaluation, for the representation of the confidence interval auxiliary lines were drawn in the hysteresis loops of hystereticity factors v_A and v_B in **Figure 16** (figures on the right column). All points of the confidence interval were considered as significant deviations, i.e., justified hystereticity. The distance from the $v = 1$ indicates hysteresis in the retention, while the "wideness" of the hystereticity loops indicates hysteresis in the selectivity. For better visualization, all chromatograms of **ABA–3** in the 2-PrOH/1-PrOH eluent system in **Figure 16D** can be seen in **Figure 15.** As all presented curves illustrate, hysteretic behavior was observed for several analytes under different chromatographic conditions. In other words, depending on the structure of the analyte and employed mobile phase, in all studied eluent systems, examples for the hysteretic behavior of ADMPC-based selector were found.

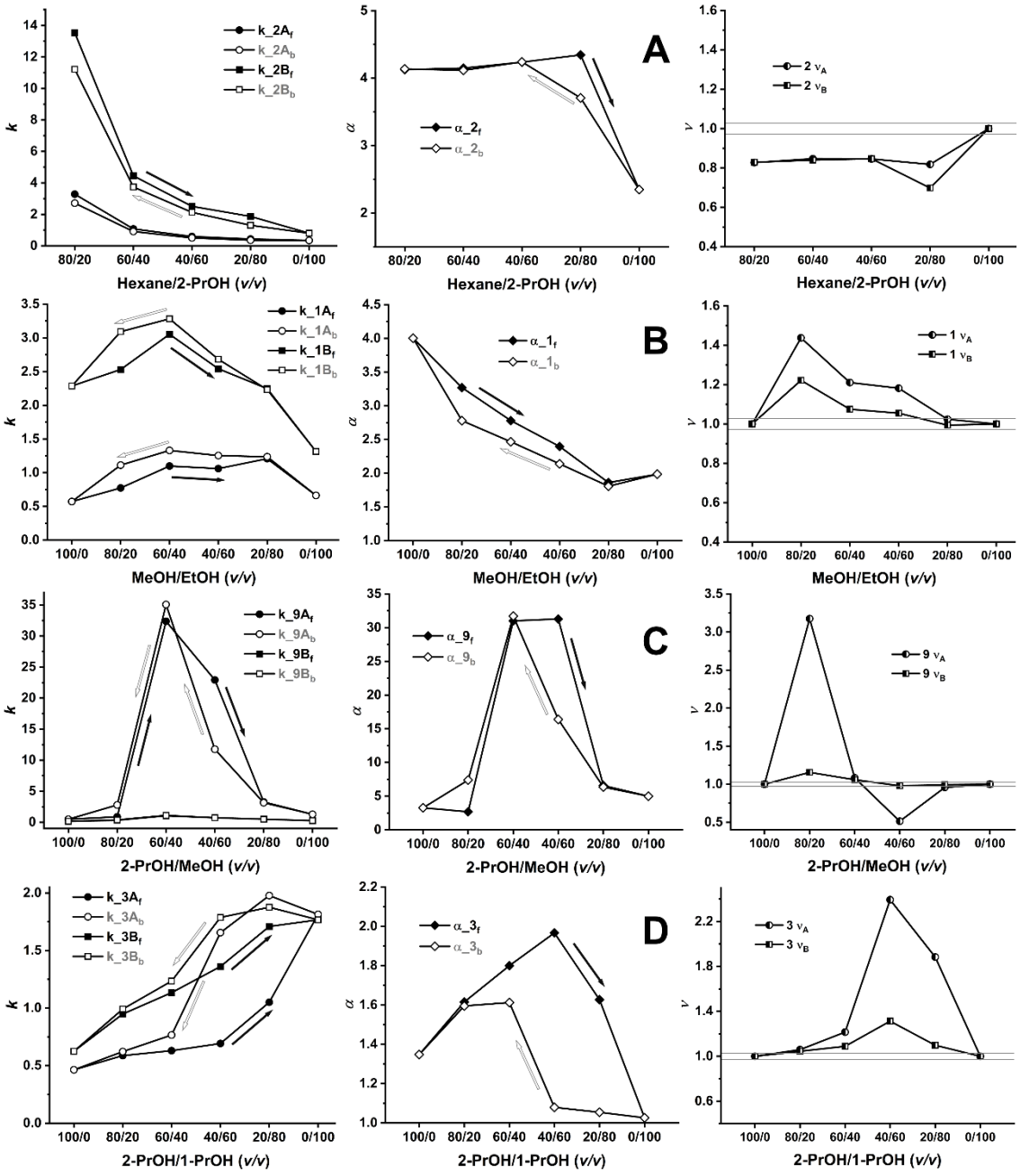

Figure 16. Hysteresis loops of **A) ABA–2**, **B) ABA–1**, **C) ABA–9**, and **D) ABA–3** applying **cA1** column

Chromatographic conditions: column, Phenomenex Lux Amylose-1; mobile phase, **A)** *n*-hexane/2-PrOH, **B)** MeOH/EtOH, **C)** 2-PrOH/MeOH, and **D)** 2-PrOH/1-PrOH; flow rate, 1.0 mL min^{-1} (0.5 mL min^{-1} in the PrOH-containing eluent systems); detection, 215 nm; temperature, 25 °C

The simplest way to characterize hystereticity is the calculation of its deviation from 1. Since either positive or negative deviation is possible, in the following we apply the absolute value for representation ($\Delta v = |v - 1|$). The highest hystereticity ($\Delta v > 1$) was observed in PO mode in the PrOH-containing eluent systems, while in the presence of MeOH, EtOH, and MeCN typically modest ($\Delta v \geq 0.3$) or low ($\Delta v < 0.3$) hystereticity was

found. In NPM (mostly at higher 2-PrOH content) low or insignificant hystereticity was observed. This approach is easily applicable to characterize hystereticity from a chromatographic point of view. However, from a mathematical point of view, it still suffers from some limitations; since it is based on a division, the scale obtained will be between zero and infinity, with 1 in the middle. Further refinement of this approach is also possible by the utilization of a logarithmic scale. The use of the logarithmic approach results in a symmetrical scale. A "tight" loop of hystereticity factors, i.e., v_A and v_B has little difference, and it indicates that hysteresis in the selectivity is low and the hysteresis affects both enantiomers in a similar manner. However, in many cases, one of the two enantiomers has a significantly higher contribution to the hysteresis, i.e., a significant hysteresis in the selectivity is present, which is depicted in the middle column of **Figure 16** as "widened" loops, indicating that there are differences between the selectivities of forward and backward directions. The right column of **Figure 16** can be interpreted as the combination of the left and middle columns: the deviation from 1 indicates the hysteresis in the retention, while the "wideness" of the loop indicates the hysteresis of selectivity (based on the configuration). The hysteresis of selectivity (based on the configuration) can be accurately and comparably presented by the log (v_A/v_B) values and information can be extracted about the percentage contribution of each enantiomer to the hysteresis. (Logarithmic and percentage values can be seen in **Table A10** with the example of the 2-PrOH/MeOH eluent system, as well as a description of calculating these values.) It is worth noting, that in the 2-PrOH/MeOH eluent at a composition of 40/60 (*v/v*), lactones have positive, while amides have negative log (v_A/v_B) values suggesting that structurally strongly related compounds can behave uniformly from a hysteretic point of view.

To investigate the effect of the PS type on hysteresis, the cellulose-based **cC1** should have been applied; however, its effectiveness did not make it possible to compare it with the **cA1** column. Fortunately, of the different DMP selectors, **cC4** was adequate for the task. In earlier studies, no or negligible hysteresis was found when applying cellulose-based CSPs [44,49,50]. In contrast to these results, significant hysteresis was found in the case of **ABA–5**. It is worth noting, that in a wider composition range applying a 2-PrOH/MeOH mobile phase system, the hysteretic behavior was only observed in the case of **ABA–5** of the studied analytes. The potential influence of immobilization on hysteresis was evaluated with the **iA1** column and 2-PrOH/MeOH eluent system, where the immobilization of the SO was found to have a marked effect on

hystereticity. Compared to the results obtained with the coated phase, markedly lower hystereticity (Δv < 0.2) was found. Not only the values of Δv were lower, but also the mobile phase composition range where the hysteresis occurred was narrower; significant hystereticity was only observed at higher MeOH contents.

5.5. Effect of temperature and assessment of thermodynamic parameters

To shed some light on the separation mechanisms, both ZIE- and PS-based CSPs were utilized for the investigation of the effects of temperature on the chromatographic parameters. A variable-temperature study was carried out with all **ATO**–analytes on four PS-based CSPs (**IA**, **IB**, **IE**, **IC**), and all **FBP** analytes on the two ion exchanger CSPs (**ZWIX(+)** and **ZWIX(–)**) in the temperature range of 10 to 50 °C in 10 °C increments. Extra 5 °C data points were also recorded in the case of **ZWIX(+)** and **ZWIX(–)** columns.

5.5.1. Thermodynamic parameters obtained for the fluorinated β³-phenylalanine derivatives with zwitterionic CSPs [76]

To make a more accurate evaluation of the calculated apparent thermodynamic parameters, WLR, and confidence intervals were calculated at a confidence level of 95%. *RSD%* values were determined at 30 °C from three parallel measurements in seven cases, both in the 100/0 and 50/50 (*v/v*) MeOH/MeCN eluent systems. *RSD%* of k_1 was lower than 1.0%, *RSD%* of α was lower than 0.5% and *RSD%* of R_S was lower than 2.5% in all cases.

Separation was observed in all cases, and baseline separation (R_S > 1.5) was achieved in most cases. In all cases on both CSPs, the retention factors decreased with increasing temperature. In general, transfer of SA from the mobile phase to the stationary phase is an exothermic process, thus k (and α) usually decrease with increasing temperature. The change in α as the function of temperature was between 14% and 28% in most cases on **ZWIX(–)** (less in MeOH, more in MeOH/MeCN 50/50 (*v/v*) mobile phases), while less on **ZWIX(+)**, between 5% and 12% (**Table A6**). However, **FBP–6** on **ZWIX(+)** showed a unique behavior. Its separation factor, α did not change significantly in the 100% MeOH mobile phase within the examined temperature range. This behavior indicates that the differences in the three-dimensional structure and solvation with temperature between the two CSPs probably contribute to this unusual effect. The resolution showed minimal variation with temperature, typically following a slight

dome-shaped curve that decreased further at higher temperatures. At first, increasing temperature may improve both peak symmetry and efficiency by improving the kinetics of separation, thus resolution can increase this way. At higher temperatures the large decrease in α compensates for the latter effect and, as a result, resolution decreases.

In addition to theoretical limitations discussed comprehensively by *Asnin* and *Stepanova* [56], the correctness of *van't Hoff* plots was examined by *Felinger et al*. [98], focusing on instrumental and experimental conditions, particularly addressing the flow rate (pressure drop across the column). They found that it affected the calculated thermodynamic parameters. It is noteworthy that the aforementioned study was conducted under achiral conditions, and ΔH^0 and ΔS^0 values were calculated. Inspired by their work, a systematic study was designed to reveal further details about the applicability of the *van't Hoff* approach in enantioselective chromatography, focusing on the $\Delta(\Delta X^0)$ apparent thermodynamic parameters. Evaluation of the effects of flow rate on these thermodynamic parameters was performed by setting 0.3, 0.6, or 0.9 mL min^{-1} flow rates and employing a constant mobile phase composition of MeOH/MeCN 50/50 (*v/v*) with FA (50 mM) and DEA (25 mM) on the **ZWIX(–)** column. Experimental data obtained for the six studied SAs using *van't Hoff* analysis are summarized in **Table 2**. Usually, the most negative $\Delta(\Delta H^0)$ and $\Delta(\Delta S^0)$ values were obtained at the lowest flow rate, but no regularity could be observed and changes were rather small. The **ZWIX(+)** column was also applied in a limited set of experiments with 0.6 and 0.9 mL min^{-1} flow rates, but no significant changes were recorded in $\Delta(\Delta H^0)$ and $\Delta(\Delta S^0)$ values. $\Delta(\Delta G^0)$ parameters were not affected by the flow rate in either case. Both $\Delta(\Delta H^0)$ and $\Delta(\Delta S^0)$ values changed in a narrow range and they were influenced more significantly by the structural peculiarities of the SAs than by the flow rate, even if the analytes are structurally closely related. All three thermodynamic parameters were more negative (as well as selectivities were larger) on **ZWIX(–)**, showing its superiority over the **ZWIX(+)** column in the enantioselective separation of **FBP** analytes.

The influence of mobile phase composition on thermodynamic parameters was also studied with eluent compositions of MeOH/MeCN containing FA (50 mM) and DEA (25 mM) using 0.6 mL min^{-1} flow rate. In the case of the **ZWIX(–)** column MeOH/MeCN 100/0, 75/25, and 50/50 (*v/v*), while in the case of the **ZWIX(+)** column 100/0, and 50/50 (*v/v*) eluent compositions were applied. The thermodynamic parameters calculated as discussed above, are summarized in **Table 2** and **Table A7**.

Table 2. Effects of flow rate and the bulk eluent composition on the thermodynamic parameters, $\Delta(\Delta H^0)$, $\Delta(\Delta S^0)$, $\Delta(\Delta G^0)$ of **FBP** analytes on **ZWIX(–)** column.

Analyte	$-\Delta(\Delta H^0)$ [kJ mol^{-1}]				
	a	**b**	**c**	**d**	**e**
FBP–1	5.43 ± 0.13	5.00 ± 0.13	4.84 ± 0.11	3.43 ± 0.14	4.27 ± 0.07
FBP–2	5.85 ± 0.14	5.14 ± 0.16	5.18 ± 0.10	3.32 ±0.15	4.43 ± 0.10
FBP–3	5.46 ± 0.16	5.21 ± 0.16	5.09 ± 0.10	3.84 ± 0.11	4.52 ± 0.12
FBP–4	5.36 ± 0.17	5.60 ± 0.14	5.28 ± 0.16	3.93 ± 0.12	4.69 ± 0.14
FBP–5	4.37 ± 0.13	4.40 ± 0.16	3.92 ± 0.08	3.33 ± 0.11	3.87 ± 0.14
FBP–6	3.77 ± 0.15	3.56 ± 0.11	2.98 ± 0.13	2.40 ± 0.13	2.87 ± 0.10
	$-\Delta(\Delta S^0)$ [J mol^{-1} K^{-1}]				
FBP–1	12.35 ± 0.44	10.87 ± 0.42	10.34 ± 0.37	8.10 ± 0.45	9.63 ± 0.24
FBP–2	13.72 ± 0.48	11.29 ± 0.54	11.46 ± 0.34	7.94 ± 0.50	10.11 ± 0.33
FBP–3	12.42 ± 0.54	11.60 ± 0.52	11.16 ± 0.35	9.36 ± 0.36	10.40 ± 0.41
FBP–4	11.84 ± 0.55	12.62 ± 0.47	11.54 ± 0.54	9.66 ± 0.40	10.77 ± 0.47
FBP–5	8.59 ± 0.44	8.68 ± 0.53	7.17 ± 0.25	7.01 ± 0.38	7.82 ± 0.47
FBP–6	7.85 ± 0.49	7.18 ± 0.37	5.27 ± 0.43	4.89 ± 0.42	5.67 ± 0.32
	$-\Delta(\Delta G^0)_{298K}$ [kJ mol^{-1}]				
FBP–1	1.75 ± 0.19	1.76 ± 0.18	1.76 ± 0.16	1.01 ± 0.19	1.40 ± 0.10
FBP–2	1.76 ± 0.20	1.77 ± 0.23	1.76 ± 0.14	0.95 ± 0.21	1.42 ± 0.14
FBP–3	1.75 ± 0.23	1.75 ± 0.22	1.76 ± 0.15	1.05 ± 0.15	1.42 ± 0.17
FBP–4	1.83 ± 0.23	1.83 ± 0.20	1.84 ± 0.23	1.05 ± 0.17	1.48 ± 0.20
FBP–5	1.81 ± 0.19	1.81 ± 0.22	1.79 ± 0.11	1.24 ± 0.16	1.54 ± 0.20
FBP–6	1.43 ± 0.21	1.42 ± 0.16	1.40 ± 0.18	0.94 ± 0.18	1.18 ± 0.13

Chromatographic conditions: column, ZWIX(–); mobile phase, all containing 25 mM DEA and 50 mM FA, **a)** MeOH/MeCN 50/50 (*v/v*); flow rate, 0.3 mL min^{-1}, **b)** MeOH/MeCN 50/50 (*v/v*); flow rate, 0.6 mL min^{-1}, **c)** MeOH/MeCN 50/50 (*v/v*); flow rate, 0.9 mL min^{-1}; **d)** MeOH/MeCN 100/0 (*v/v*); flow rate, 0.6 mL min^{-1}, **e)** MeOH/MeCN 75/25 (*v/v*); flow rate, 0.6 mL min^{-1}; detection, 262 nm; temperature, 5–50 °C.

In all five cases, a clear tendency can be seen between the MeCN content and the $\Delta(\Delta H^0)$, $\Delta(\Delta S^0)$, and $\Delta(\Delta G^0)$ values as they became more negative with increasing MeCN content. Minor differences in the parameters among the stationary phases suggest comparable separation characteristics, except for **FBP–6**, which showed no significant change in selectivity as a function of temperature on **ZWIX(+)**. This may be attributed to different electronic effects, including changes in electron distribution and polar properties, due to trifluorination of the methyl group on the phenyl ring. These effects are more pronounced when stronger Coulomb interactions are less likely to form, e.g., as when a lower ratio of MeCN is present in the eluent. To reveal the contribution of the enthalpy and entropy to the enantioseparation, $Q = \Delta(\Delta H^0) / [T \times \Delta(\Delta S^0)$; T = 298 K] values were also calculated

with confidence intervals (**Table 3**). The interpretation of Q values is that when $|Q| > 1$ then the separation is enthalpically driven, and if $|Q| < 1$ then the separation is entropically driven. Both $\Delta(\Delta H^0)$ and $\Delta(\Delta S^0)$ values of **FBP–6** have similar confidence intervals as of other analytes in the MeOH/MeCN 50/50 (*v/v*) eluent system. In the case of **FBP–6** on the **ZWIX(+)** column in 100% MeOH, the confidence interval of Q was too large and made it uncertain to decide whether the separation was driven by enthalpy or entropy (**Table 3**), which emphasizes the importance of the calculation of confidence intervals. It is especially true in the case of calculated values where the propagation of error further increases the default error of measurement. In all other cases, separations were enthalpically driven.

Table 3. Effects of eluent composition on the $\Delta(\Delta H^0)$ / [T*$\Delta(\Delta S^0)$] ratio of **FBP** analytes on **ZWIX(–)** and **ZWIX(+)** column

Analyte	***Q***		
	Column: **ZWIX(–)**		
	a	**b**	**c**
1	1.42 ± 0.10	1.49 ± 0.04	1.54 ± 0.07
2	1.40 ± 0.11	1.47 ± 0.06	1.53 ± 0.09
3	1.38 ± 0.07	1.46 ± 0.07	1.51 ± 0.08
4	1.36 ± 0.07	1.46 ± 0.08	1.49 ± 0.07
5	1.59 ± 0.10	1.66 ± 0.12	1.70 ± 0.12
6	1.65 ± 0.17	1.70 ± 0.11	1.66 ± 0.10
	Column: **ZWIX(+)**		
1	1.61 ± 0.15	No data	1.39 ± 0.11
2	1.43 ± 0.11	No data	1.37 ± 0.13
3	1.25 ± 0.14	No data	1.33 ± 0.13
4	1.19 ± 0.12	No data	1.31 ± 0.13
5	1.81 ± 0.24	No data	1.45 ± 0.07
6	–*	No data	1.80 ± 1.00

Chromatographic conditions: columns, ZWIX(–) and ZWIX(+); mobile phases, all containing 25 mM DEA and 50 mM FA, **a)** MeOH/MeCN 100/0 (*v/v*); **b)** MeOH/MeCN 75/25 (*v/v*); **c)** MeOH/MeCN 50/50 (*v/v*); flow rate, 0.6 mL min^{-1}; detection, 262 nm. $Q = \Delta(\Delta H^0)$ / [T*$\Delta(\Delta S^0)$; T = 298 K]. *: no significant change in selectivity beyond the margin of measurement error.

Tanács et al. discussed the importance of the solvation of SA and SO in the case of ion exchanger-based CSPs [99]. The electrostatic forces formed between SO and SA were found to be strongly affected by the thickness of solvation spheres developed around the charged species. Since MeCN possesses lower solvation power for the chargeable sites of SA and SO, increasing its ratio in the mobile phase results in an

enhanced Coulomb attraction. In the case of ZIE CSPs, adsorption relates to electrostatic forces which, in turn, are affected by the solvation shells. Therefore, the solvent can influence the adsorption and it triggers the overall stereorecognition, as discussed in this section.

5.5.2. Thermodynamic parameters obtained for the amino, thio, and oxy analogs of monoterpene lactone derivatives with PS-based CSPs [75]

Thermodynamic aspects of all **ATO** analytes were investigated on **IA**, **IB**, **IE**, and **IC** columns in NPM using *n*-hexane/EtOH/DEA 80/20/0.1 (*v/v/v*) eluent composition. Separation was observed in most cases; however, a few exceptions were also found. In general, both the retention factor (k_1) and the selectivity (α) decreased with increasing temperature. In contrast, an increase in selectivity was recorded in the case of **ATO–5** on **IA** and **IB**, **ATO–2** and **7** on **IC**, and **ATO–1** on **IE**. According to data listed in **Table 4**, both negative and positive values of $\Delta(\Delta H^0)$ and $\Delta(\Delta S^0)$ were present. Negative values indicate a stronger complex formation between the SO and the second-eluting SA. *Q* values were also calculated and revealed that in these cases, separations were driven by enthalpy, while the selectivity decreased with increasing temperature. It is worth noting that the large confidence intervals of *Q* values sometimes (especially when *Q* was close to 1) made it uncertain to decide whether the enantioseparations were enthalpically or entropically driven. When both $\Delta(\Delta H^0)$ and $\Delta(\Delta S^0)$ were positive, selectivity increased with increasing temperature, while *Q* revealed entropically driven enantioseparations in the case of all four analytes. However, it could not be clearly stated in the case of **ATO–2** on **IC** (and **IB**, see both in **Table A8**) due to the calculated confidence intervals or too few data points (a.k.a. enantioseparations on different temperatures).

Table 4. Thermodynamic parameters, $\Delta(\Delta H^0)$, $\Delta(\Delta S^0)$, $\Delta(\Delta G^0)$, and Q values of **ATO** analytes on the amylose-based **IA** and **IE** columns.

Analyte	Column: **IA**			
	$-\Delta(\Delta H^0)$ **[kJ mol^{-1}]**	$-\Delta(\Delta S^0)$ **[J mol^{-1} K^{-1}]**	$-\Delta(\Delta G^0)_{298K}$ **[kJ mol^{-1}]**	Q
1	4.07 ± 0.25	11.71 ± 0.83	0.58 ± 0.35	1.17 ± 0.11
2	8.24 ± 0.20	20.75 ± 0.67	2.05 ± 0.28	1.33 ± 0.05
3	4.82 ± 0.22	13.49 ± 0.72	0.80 ± 0.31	1.20 ± 0.08
4	5.02 ± 0.24	14.00 ± 0.80	0.85 ± 0.34	1.20 ± 0.09
5	–1.32 ± 0.07	–5.53 ± 0.23	0.33 ± 0.10	0.80 ± 0.05
6	3.61 ± 0.29	11.53 ± 0.98	0.18 ± 0.41	1.05 ± 0.12
7	1.95 ± 0.28	5.85 ± 0.97	0.20 ± 0.40	1.12 ± 0.25
8	0.68 ± 0.04	1.60 ± 0.14	0.20 ± 0.06	1.42 ± 0.16
9	1.25 ± 0.26	1.74 ± 0.88	0.73 ± 0.37	2.41 ± 1.31
10	0.50 ± 0.17	1.22 ± 0.56	0.14 ± 0.24	1.39 ± 0.78
	Column: **IE**			
1	–0.75 ± 0.10	–2.97 ± 0.33	0.13 ± 0.14	0.85 ± 0.15
2	n.s.	n.s.	n.s.	n.s.
3	1.36 ± 0.06	4.23 ± 0.22	0.10 ± 0.09	1.08 ± 0.07
4	1.01 ± 0.20	2.63 ± 0.66	0.23 ± 0.28	1.29 ± 0.41
5	6.39 ± 0.19	16.41 ± 0.63	1.50 ± 0.27	1.31 ± 0.06
6	3.63 ± 0.14	9.34 ± 0.45	0.84 ± 0.19	1.30 ± 0.08
7	2.17 ± 0.28	6.93 ± 0.93	0.11 ± 0.40	1.05 ± 0.20
8	2.58 ± 0.08	6.20 ± 0.27	0.73 ± 0.12	1.40 ± 0.08
9	2.36 ± 0.16	6.21 ± 0.54	0.51 ± 0.23	1.27 ± 0.14
10	3.37*	11.49*	0.06*	0.98*

Chromatographic conditions: column, Chiralpak IA and IE; mobile phase, *n*-hexane/EtOH/DEA 80/20/0.1 (*v/v/v*); flow rate, 1.0 mL min^{-1}; detection, 220 nm; temperature, 10–50 °C. $Q = \Delta(\Delta H^0) / [T^*\Delta(\Delta S^0)]$; T = 298 K]. n.s.: no separation observed. *: not enough data points in the temperature range to calculate confidence intervals.

Of the four CSPs, the most negative $\Delta(\Delta H^0)$ and $\Delta(\Delta S^0)$ values were obtained most frequently on the amylose-based **IA** and **IE** columns. Regarding the effect of the phenylcarbamate groups of the SOs, slight differences can be found between the amylose-based DMPC **IA** and dichlorophenylcarbamate-modified **IE** SOs, while more negative $\Delta(\Delta H^0)$ and $\Delta(\Delta S^0)$ values were obtained in the case of the cellulose-based dichlorophenylcarbamate **IC**, than on the DMPC-modified **IB** SO (**Table A8**).

6. Summary

In my research work, the separation performance of different types of selectors and selectands was investigated utilizing zwitterionic ion exchanger- and polysaccharide-type CSPs. Enantioseparations of fluorinated β^3-phenylalanines, amino, thio, oxy, azole, and benzoazole analogs of monoterpene lactone derivatives were carried out utilizing various mobile phase compositions in NP, PO, and PI modes at different temperatures to characterize the effects of the chromatographic environment on enantioseparation and determine thermodynamic parameters.

1. The effect of mobile phase composition in the case of *Cinchona* alkaloid-based CSPs was studied with the enantioseparation of fluorinated β^3-phenylalanine derivatives in PI mode on zwitterionic CSPs. As a tendency, both retention and selectivity increased with increasing amount of aprotic MeCN relative to the protic MeOH in the bulk eluent composition, indicating the importance of stronger solvation effect of MeOH. However, selectivity and resolution usually changed according to a maximum curve, reaching the maximum at a composition of MeOH/MeCN 50/50 or 25/75 (*v/v*). All analytes were separated with good selectivity at a moderate or low ratio of MeCN in the bulk mobile phase. In contrast, the applied anion exchanger columns were found to be unsuitable for the enantioseparation of these amino acid derivatives.

   Different PS-based columns or eluent compositions were needed to separate the enantiomers of all monoterpene lactone derivatives in NPM. When applying PO mode with neat solvents, all azole and benzoazole analogs were separated in MeCN. The nature of the alcohol modifier can greatly influence the separation in NP mode. Even EEO reversals were observed when an alcohol of different nature or concentration was present in the mobile phase, while the retention showed typical NP behavior as the retention factor decreased with increasing alcohol concentrations. In most cases, retention factors, applying only neat alcohols in PO mode, decreased in the order EtOH > MeOH > 1-PrOH > 2-PrOH following their polarity, except for EtOH.
2. The effect of the nature and concentration of mobile phase additives was also studied on both types of *Cinchona* alkaloid-based CSPs with the ratio of acid to base additives set to 2:1. The elution strength of base additives was TEA < DEA < EA. Retention decreased with the increasing counterion concentration and it could be

described with the simple stoichiometric displacement model. Neither the nature of the base nor the concentration of additives had a marked effect on selectivity and resolution.

In the case of polysaccharide-based CSPs, additives had slight effects on the chromatographic parameters. An exception was observed for two of the most basic monoterpene derivatives when only FA was added into the mobile phase both in NP and PI modes. In these cases, the dissociation or ion pair formation was suggested to describe the observed chromatographic behavior. The impact of the additives has been shown to be minimal when using PS-based CSPs; instead, their requirement depends on the acid-base characteristics of the studied analytes.

3. The structure of the analytes and selectors variedly affected the enantioseparations. In contrast with the enantioseparations carried out on macrocyclic glycopeptide-based CSPs, both non-fluorinated phenylalanine derivatives and those fluorinated at different positions showed no vital differences in their chromatographic properties. The only exception is **FBP–6** had slightly lower selectivities at higher MeCN ratios than other phenylalanines. This suggests that the trifluorination of the methyl group attached to the phenyl ring has a pronounced effect on the enantioselectivity. EEOs were determined in all cases with $R < S$ for all **FBP–** analytes in all cases on the **ZWIX(–)** column, and $S < R$ on the **ZWIX(+)** column without any exception. Comparing the columns, the chromatographic parameters were larger on **ZWIX(–)** CSP than on **ZWIX(+)**.

   Coated and immobilized-type polysaccharide-based CSPs with the same selector showed small differences in most cases, with retentions being lower, while enantioselectivities and resolutions being higher on the coated-type column. Considering polysaccharides, the amylose-based CSPs offered a better fit for the studied analytes than the cellulose-based CSPs, independently of the applied chromatographic mode. Retention of **ATO** analytes on PS-based CSPs showed a correlation with the size of the analytes in NPM. On the contrary, the nature of the polar solvent in POM affects retention and enantiorecognition in several ways, resulting in pronounced differences, even in the case of structurally related compounds. The EEO of monoterpene lactone derivatives were varied, seemingly in an unsystematic way. Varying the nature of selectors or the nature and concentration of bulk solvent and additives, differences in EEOs were observed in several cases even in the case of structurally closely related SOs and SAs.

4. Hysteretic behavior of PS-based CSPs was found in several cases. The hysteretic behavior causes changes in retention times independently for each enantiomer. Since both the degree and the direction of the change in retention time can be different, enantioselectivity may stay constant or hysteresis of the enantioselectivity also happens. Moreover, EEO reversals can also happen during the hysteresis. The hystereticity factor (v) describes the hysteresis of the retention factor and it is defined based on the direction from which the given composition is approached. To decide whether hysteresis is present or not, simplified confidence intervals of hystereticity were calculated and hysteresis loops were constructed. The hysteresis of selectivity (based on the configuration) can be accurately and comparably presented by log (v_A/v_B) values. Our research group was the first to propose this novel evaluation methodology for hysteresis data, including the calculation of confidence intervals, hysteresis of selectivity, percentage contribution of an enantiomer to the overall hysteresis, and the logarithmic approach. The coated-type amylose-based ADMPC SO showed hysteresis for all azole and benzoazole analogs. The highest hysteresis was observed in PO mode in binary eluent systems containing 1- and 2-PrOH, while in the presence of MeOH, EtOH, and MeCN typically modest or low hysteresis was found. In NP mode (mostly at higher 2-PrOH content) low or insignificant hystereticity was observed. The immobilized-type ADMPC SO from the same manufacturer was also tested for hysteresis. Compared to the coated-type CSP, markedly lower hysteresis was found. A coated-type cellulose-based column was also utilized and hysteresis was found in a single case. The hysteresis effect of polysaccharide-based CSPs needs special attention, but its undesirable effects can be prevented with proper column handling.
5. The effect of temperature was investigated for both types of CSPs in the temperature range of 10–50 °C on the ZIE CSPs. In all cases, retention factors and selectivities (except for **FBP–6**) decreased with increasing temperature. The apparent thermodynamic parameters were calculated by the *van't Hoff* equation. Confidence intervals, rarely applied in the evaluation of *van't Hoff* plots, were calculated, which helped the evaluation of data obtained. Both $\Delta(\Delta H^0)$ and $\Delta(\Delta S^0)$ values were negative, indicating that the separations were enthalpically driven. These values changed in a narrow range and they were influenced more significantly by the structural peculiarities of the SAs than by the flow rate, even if the analytes are structurally closely related. All three thermodynamic parameters were more negative

(as well as the selectivities were larger) on **ZWIX(–)**, showing its superiority over the **ZWIX(+)** column in the enantioselective separation of **FBP** analytes. A clear tendency can be seen between the MeCN content and the thermodynamic parameters when changing the MeCN ratio in the bulk eluent. Relatively small differences in the parameters between the analytes indicate similar characteristics in the separation process, except for **FBP–6**, which showed no significant change in selectivity as a function of temperature on **ZWIX(+)** in 100% MeOH mobile phase.

In the case of PS-based CSPs, in most cases, both retention and selectivity decreased with increasing temperature and amylose-based CSPs showed more negative $\Delta(\Delta H^0)$ and $\Delta(\Delta S^0)$ values than cellulose-based CSPs. In addition, only slight differences were found when the SOs with different phenylcarbamate groups were compared. The separation was enthalpically driven. However, on amylose-based CSPs, in some cases, retention decreased while selectivity increased with increasing temperature. At the same time, both $\Delta(\Delta H^0)$ and $\Delta(\Delta S^0)$ were positive and *Q* revealed entropically driven enantioseparation. The apparent thermodynamic parameters of the monoterpene analogs and their structures were more diverse in comparison to those of the phenylalanine derivatives.

References

[1] L. R. Snyder, J. J. Kirkland, J. W. Dolan, Introduction to Modern Liquid Chromatography, 3rd ed, John Wiley & Sons, Inc., Hoboken, NJ, 2010.

[2] G.K.E. Scriba, ed., Chiral Separations, Springer New York, New York, NY, 2019.

[3] M. Lämmerhofer, J Chromatogr A 1217 (2010) 814–856.

[4] R. Berkecz, G. Németi, A. Péter, I. Ilisz, Molecules 26 (2021) 4648.

[5] R. Kimura, H. Tsujimura, M. Tsuchiya, S. Soga, N. Ota, A. Tanaka, H. Kim, Sci Rep 10 (2020) 804

[6] S.J. Jaag, Y. Valadbeigi, T. Causon, H. Gross, M. Lämmerhofer, Anal Chem 96 (2024) 2666–2675.

[7] M. Tswett, Ber Dtsch Bot Ges (1906) 384–393.

[8] J. Livengood, Studies in History and Philosophy of Science Part A 40 (2009) 57–69.

[9] G.M. Henderson, H.G. Rule, Nature 141 (1938) 917–918.

[10] C. Roussel, P. Piras, I. Heitmann, Biomedical Chromatography 11 (1997) 311–316.

[11] L.H. Easson, E. Stedman, Biochemical Journal 27 (1933) 1257–1266.

[12] M. Kotake, T. Sakan, N. Nakamura, S. Senoh, J Am Chem Soc 73 (1951) 2973–2974.

[13] C.E. Dalgliesh, Journal of the Chemical Society (Resumed) (1952) 3940.

[14] W.H. Pirkle, T.C. Pochapsky, Chem Rev 89 (1989) 347–362.

[15] V.A. Davankov, Chirality 9 (1997) 99–102.

[16] A. Berthod, Anal Chem 78 (2006) 2093–2099.

[17] A. Berthod, ed., Chiral Recognition in Separation Methods, Springer Berlin Heidelberg, Berlin, Heidelberg, 2010.

[18] C. V. Hoffmann, R. Pell, M. Lämmerhofer, W. Lindner, Anal Chem 80 (2008) 8780–8789.

[19] N. Grubhofer, L. Schleith, Naturwissenschaften 40 (1953) 508–508.

[20] N. Grubhofer, L. Schleith, Hoppe Seylers Z Physiol Chem 296 (1954) 262–6.

[21] C. Pettersson, J Chromatogr A 316 (1984) 553–567.

[22] C. Rosini, C. Bertucci, D. Pini, P. Altemura, P. Salvadori, Tetrahedron Lett 26 (1985) 3361–3364.

[23] M. Lämmerhofer, W. Lindner, J Chromatogr A 741 (1996) 33–48.

[24] A. Mandl, L. Nicoletti, M. Lämmerhofer, W. Lindner, J Chromatogr A 858 (1999) 1–11.

[25] C. V. Chandarana, J. Rejji, Journal of Analytical Chemistry 78 (2023) 267–293.

[26] K. Schmitt, U. Woiwode, M. Kohout, T. Zhang, W. Lindner, M. Lämmerhofer, J Chromatogr A 1569 (2018) 149–159.

[27] C. V. Hoffmann, M. Laemmerhofer, W. Lindner, J Chromatogr A 1161 (2007) 242–251.

[28] C. V. Hoffmann, R. Reischl, N.M. Maier, M. Lämmerhofer, W. Lindner, J Chromatogr A 1216 (2009) 1147–1156.

[29] L. Asnin, J. Herciková, W. Lindner, Y. Klimova, D. Ziganshina, E. Reshetova, M. Kohout, Chirality 34 (2022) 1065–1077.

[30] H. Krebs, J.A. Wagner, J. Diewald, Chem Ber 89 (1956) 1875–1883.

[31] G. Hesse, R. Hagel, Chromatographia 6 (1973) 277–280.

[32] Y. Okamoto, M. Kawashima, K. Hatada, J Am Chem Soc 106 (1984) 5357–5359.

[33] B. Chankvetadze, J Chromatogr A 1269 (2012) 26–51.

[34] L. Mosiashvili, L. Chankvetadze, T. Farkas, B. Chankvetadze, J Chromatogr A 1317 (2013) 167–174.

[35] G. Jibuti, A. Mskhiladze, N. Takaishvili, M. Karchkhadze, L. Chankvetadze, T. Farkas, B. Chankvetadze, J Sep Sci 35 (2012) 2529–2537.
[36] K.S.S. Dossou, P. Chiap, B. Chankvetadze, A. Servais, M. Fillet, J. Crommen, J Sep Sci 33 (2010) 1699–1707.
[37] B. Chankvetadze, TrAC Trends in Analytical Chemistry 122 (2020) 115709.
[38] B. Chankvetadze, C. Yamamoto, Y. Okamoto, J Chromatogr A 922 (2001) 127–137.
[39] S. Materazzo, S. Carradori, R. Ferretti, B. Gallinella, D. Secci, R. Cirilli, J Chromatogr A 1327 (2014) 73–79.
[40] R. Ferretti, L. Zanitti, A. Casulli, R. Cirilli, J Sep Sci 39 (2016) 1418–1424.
[41] G.K.E. Scriba, TrAC Trends in Analytical Chemistry 120 (2019) 115639.
[42] N. Beridze, E. Tsutskiridze, N. Takaishvili, T. Farkas, B. Chankvetadze, Chromatographia 81 (2018) 611–621.
[43] D. Tanács, T. Orosz, Z. Szakonyi, T.M. Le, F. Fülöp, W. Lindner, I. Ilisz, A. Péter, J Chromatogr A 1621 (2020) 461054.
[44] S. Horváth, G. Németh, J Chromatogr A 1568 (2018) 149–159.
[45] S. Horváth, Z. Eke, G. Németh, J Chromatogr A 1625 (2020) 461280.
[46] S. Horváth, Z. Eke, G. Németh, J Chromatogr A 1673 (2022) 463052.
[47] S. Horváth, H.H. Nguyen Thuy, Z. Eke, G. Németh, J Chromatogr A 1705 (2023) 464161.
[48] G. Subramanian, Chiral separation techniques: A practical approach, WILEY-VCH Verlag GmbH & Co. KGaA, Winheim, Germany, 2007.
[49] M. Foroughbakhshfasaei, M. Dobó, F. Boda, Z.-I. Szabó, G. Tóth, Molecules 27 (2021) 111.
[50] M. Dobó, M. Foroughbakhshfasaei, P. Horváth, Z.-I. Szabó, G. Tóth, J Chromatogr A 1662 (2022) 462741.
[51] M. Maisuradze, G. Sheklashvili, A. Chokheli, I. Matarashvili, T. Gogatishvili, T. Farkas, B. Chankvetadze, J Chromatogr A 1602 (2019) 228–236.
[52] I. Matarashvili, G. Kobidze, A. Chelidze, G. Dolidze, N. Beridze, G. Jibuti, T. Farkas, B. Chankvetadze, J Chromatogr A 1599 (2019) 172–179.
[53] R. Sardella, E. Camaioni, A. Macchiarulo, A. Gioiello, M. Marinozzi, A. Carotti, TrAC Trends in Analytical Chemistry 122 (2020) 115703.
[54] T.L. Chester, J.W. Coym, J Chromatogr A 1003 (2003) 101–111.
[55] E. Caiali, V. David, H.Y. Aboul-Enein, S.C. Moldoveanu, J Chromatogr A 1435 (2016) 85–91.
[56] L.D. Asnin, M. V. Stepanova, J Sep Sci 41 (2018) 1319–1337.
[57] J.N. Miller, J.C. Miller, R.D. Miller, Statistics and chemometrics for analytical chemistry, 7th ed, Pearson Education Limited, Harlow, United Kingdom, 2018.
[58] C. Zaiontz, https://real-statistics.com/multiple-regression/weighted-linear-regression/weighted-regression-basics/ (accessed 2024 August).
[59] C.R. McCudden, V.B. Kraus, Clin Biochem 39 (2006) 1112–1130.
[60] V. Singh, R.K. Rai, A. Arora, N. Sinha, A.K. Thakur, Sci Rep 4 (2014) 3875.
[61] N. N. Riaz, Fazal-ur-Rehman M, M. M. Ahmad, Med Chem (Los Angeles) 7 (2017) 302–307.
[62] J. Wang, M. Sánchez-Roselló, J.L. Aceña, C. del Pozo, A.E. Sorochinsky, S. Fustero, V.A. Soloshonok, H. Liu, Chem Rev 114 (2014) 2432–2506.
[63] I. Ojima, Fluorine in medicinal chemistry and chemical biology, John Wiley & Sons, Ltd., Chichester, United Kingdom, 2009.
[64] K. Kalíková, T. Šlechtová, E. Tesařová, Separations 3 (2016) 30

[65] B. Ivanescu, A. Miron, A. Corciova, J Anal Methods Chem 2015 (2015) 1–21.
[66] K.N. Gangadhar, M.J. Rodrigues, H. Pereira, H. Gaspar, F.X. Malcata, L. Barreira, J. Varela, Mar Drugs 18 (2020) 567.
[67] C. Vizetto-Duarte, L. Custódio, K.N. Gangadhar, J.H.G. Lago, C. Dias, A.M. Matos, N. Neng, J.M.F. Nogueira, L. Barreira, F. Albericio, A.P. Rauter, J. Varela, Phytomedicine 23 (2016) 550–557.
[68] J. Silva, C. Alves, A. Martins, P. Susano, M. Simões, M. Guedes, S. Rehfeldt, S. Pinteus, H. Gaspar, A. Rodrigues, M.I. Goettert, A. Alfonso, R. Pedrosa, Int J Mol Sci 22 (2021) 1888.
[69] J.R. Woods, H. Mo, A.A. Bieberich, T. Alavanja, D.A. Colby, Medchemcomm 4 (2013) 27–33.
[70] M. Hossain, Science Journal of Chemistry 6 (2018) 83.
[71] J. Pérez-Villanueva, A. Romo-Mancillas, A. Hernández-Campos, L. Yépez-Mulia, F. Hernández-Luis, R. Castillo, Bioorg Med Chem Lett 21 (2011) 7351–7354.
[72] S. Shahmohammadi, F. Fülöp, E. Forró, Molecules 25 (2020) 5990.
[73] T.M. Le, P. Bérdi, I. Zupkó, F. Fülöp, Z. Szakonyi, Int J Mol Sci 19 (2018) 3522.
[74] G. Németi, R. Berkecz, T.M. Le, Z. Szakonyi, A. Péter, I. Ilisz, J Chromatogr A 1717 (2024) 464660.
[75] A. Bajtai, G. Németi, T.M. Le, Z. Szakonyi, A. Péter, I. Ilisz, J Chromatogr A 1672 (2022) 463050.
[76] G. Németi, R. Berkecz, S. Shahmohammadi, E. Forró, W. Lindner, A. Péter, I. Ilisz, J Chromatogr A 1670 (2022) 462974.
[77] R. Berkecz, A. Sztojkov-Ivanov, I. Ilisz, E. Forró, F. Fülöp, M.H. Hyun, A. Péter, J Chromatogr A 1125 (2006) 138–143.
[78] A. Sztojkov-Ivanov, L. Lázár, F. Fülöp, D.W. Armstrong, A. Péter, Chromatographia 64 (2006) 89–94.
[79] I. Ilisz, N. Grecsó, R. Papoušek, Z. Pataj, P. Barták, L. Lázár, F. Fülöp, W. Lindner, A. Péter, Amino Acids 47 (2015) 2279–2291.
[80] D. Tanács, R. Berkecz, S. Shahmohammadi, E. Forró, D.W. Armstrong, A. Péter, I. Ilisz, J Pharm Biomed Anal 219 (2022) 114912.
[81] I. Ilisz, Z. Gecse, G. Lajkó, M. Nonn, F. Fülöp, W. Lindner, A. Péter, J Chromatogr A 1384 (2015) 67–75.
[82] T. O'Brien, L. Crocker, R. Thompson, K. Thompson, P.H. Toma, D.A. Conlon, B. Feibush, C. Moeder, G. Bicker, N. Grinberg, Anal Chem 69 (1997) 1999–2007.
[83] C. Xiang, G. Liu, S. Kang, X. Guo, B. Yao, W. Weng, Q. Zeng, J Chromatogr A 1218 (2011) 8718–8721.
[84] K.C. Tok, M. Gumustas, G. Jibuti, H.S. Suzen, S.A. Ozkan, B. Chankvetadze, Molecules 25 (2020) 5865.
[85] L. Thungerg, J. Hashemi, S. Andersson, Journal of Chromatography B 875 (2008) 72–80.
[86] J. Shen, T. Ikai, Y. Okamoto, J Chromatogr A 1363 (2014) 51–61.
[87] I. Ilisz, N. Grecsó, M. Palkó, F. Fülöp, W. Lindner, A. Péter, J Pharm Biomed Anal 98 (2014) 130–139.
[88] W. M. Haynes, CRC Handbook of Chemistry and Physics, 97th Edition, CRC Press, Boca Raton, FL, 2016.
[89] W. Kopaciewicz, M.A. Rounds, J. Fausnaugh, F.E. Regnier, J Chromatogr A 266 (1983) 3–21.
[90] B. Sellergren, K.J. Shea, J Chromatogr A 654 (1993) 17–28.

[91] N. Grecsó, E. Forró, F. Fülöp, A. Péter, I. Ilisz, W. Lindner, J Chromatogr A 1467 (2016) 178–187.
[92] Y. He, Y. Wu, L. Cheng, S. He, Q. Wang, H. Wang, Y. Ke, Sep Sci Plus 1 (2018) 351–358.
[93] A. Mskhiladze, M. Karchkhadze, A. Dadianidze, S. Fanali, T. Farkas, B. Chankvetadze, Chromatographia 76 (2013) 1449–1458.
[94] T. Wang, R.M. Wenslow, J Chromatogr A 1015 (2003) 99–110.
[95] R. M. Wenslow, T. Wang, Anal Chem 73 (2001) 4190–4195.
[96] Phenomenex Column protection guide (ver. 1009)
[97] Instruction manual for Chiralpak AD-H (07/2013LE)
[98] A. Sepsey, É. Horváth, M. Catani, A. Felinger, J Chromatogr A 1611 (2020) 460594.
[99] D. Tanács, T. Orosz, I. Ilisz, A. Péter, W. Lindner, J Chromatogr A 1648 (2021) 462212.

Acknowledgments

I would like to express my gratitude to my supervisor, Professor István Ilisz, Head of the Institute of Pharmaceutical Analysis, for his invaluable guidance and for providing me with the opportunity to make my M.Sc. and Ph.D. work. I am grateful to Professor Antal Péter for his mentorship, who also guided my work. I also would like to thank Dr. Tímea Orosz, a former Ph.D. student, who guided me in my initial years in the research group. Their mentorship and support were essential to the advancement of my knowledge and research in this field.

I would like to thank my colleagues, Dr. Attila Bajtai, Dr. Dániel Tanács, Dr. Tímea Körmöczi, Dr. Róbert Berkecz, and Gabriella Vasas for their advice in diverse fields, Melinda Guba and Dr. Dániel Ozsvár for their help with my measurements, as well as to all other members of the Institute of Pharmaceutical Analysis.

I also want to thank Professor Árpád Molnár for proofreading my thesis.

I would like to express my sincerest gratitude to my parents and sister for their support and encouragement.

This work was supported by UNKP–22–3–SZTE–156 New National Excellence Program of the Ministry for Culture and Innovation from the source of the National Research, Development and Innovation Fund, and by the National Research, Development and Innovation Office – NKFIA through project K137607. Project no. TKP2021–EGA–32 has been implemented with the support provided by the Ministry of Culture and Innovation of Hungary from the National Research, Development and Innovation Fund, financed under the TKP2021–EGA funding scheme.

Appendix

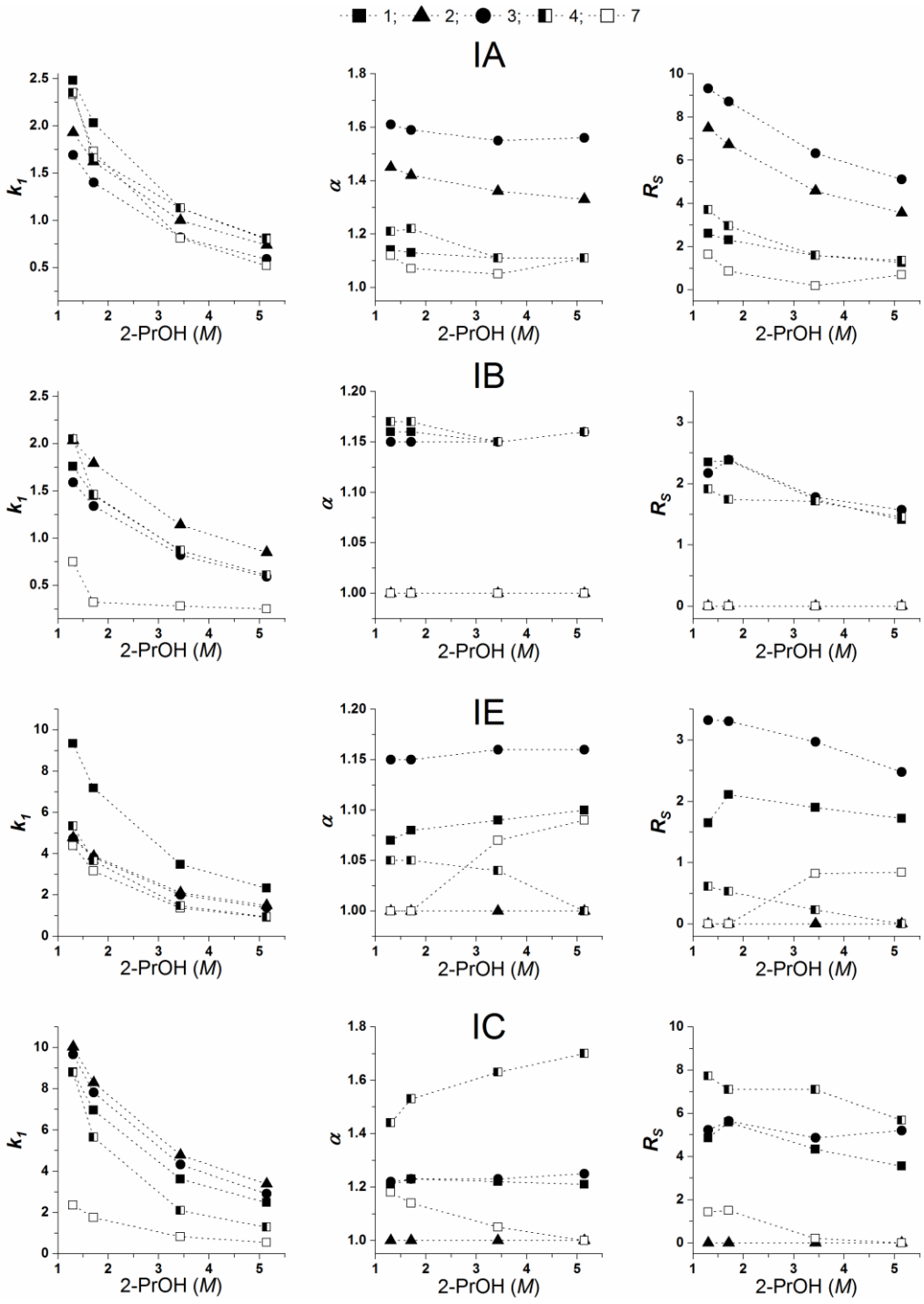

Figure A1. Effects of the concentration of the alcohol modifier 2-PrOH on the chromatographic parameters of **ATO–1-4** and **7** analytes in NPM applying **IA**, **IB**, **IE**, and **IC** columns

Chromatographic conditions: columns, Chiralpak IA, IB, IE, and IC; mobile phase, *n*-hexane/2-PrOH/DEA, all containing 0.1 *v*% DEA; the concentration of 2-PrOH: 1.30, 1.71, 3.43, and 5.14 M; flow rate, 1.0 mL min^{-1}; detection, 220 nm; temperature, 25 °C

Table A1. Effects of selector immobilization on the chromatographic parameters in the enantioseparation of **ATO–5**, **6**, **8**, and **9** in NPM applying coated (**cA1**) and immobilized (**iA1**) ADMPC-based CSPs.

Analyte		cA1	iA1
5	k_1	3.38	4.25
	α	1.22	1.15
	R_S	2.45	1.83
	EEO	A < B	A < B
6	k_1	3.27	3.42
	α	1.00	1.07
	R_S	0.00	1.10
	EEO	-	B < A
8	k_1	0.96	1.20
	α	6.07	4.35
	R_S	16.57	8.69
	EEO	B < A	B < A
9	k_1	0.86	1.20
	α	5.42	4.50
	R_S	17.95	17.20
	EEO	B < A	B < A

Chromatographic conditions: columns, Phenomenex Lux Amylose-1 (coated, **cA1**) and i-Amylose-1 (immobilized, **iA1**); mobile phase, *n*-hexane/2-propanol 80/20 *v/v*; flow rate, 1.0 mL min^{-1}; detection, 215 nm; temperature, 25 °C

Table A2. Effects of selector immobilization on the chromatographic parameters in the enantioseparation of azole analogs of monoterpene lactones and amides in POM applying coated (**cA1**) and immobilized (**iA1**) ADMPC-based CSPs.

Analyte		Mobile phase and column type					
		EtOH		1-PrOH		2-PrOH	
		cA1	iA1	cA1	iA1	cA1	iA1
5	k_1	2.14	0.85	0.91	1.58	0.69	0.91
	α	1.00	1.15	1.00	1.00	1.10	1.00
	R_S	0.00	1.05	0.00	0.00	0.70	0.00
	EEO	-	A < B	-	-	B < A	-
6	k_1	1.64	0.98	0.83	1.48	0.39	0.90
	α	1.32	1.20	1.48	1.10	1.18	1.00
	R_S	4.18	1.82	4.84	1.27	1.12	0.00
	EEO	B < A	B < A	B < A	B < A	A < B	-
8	k_1	0.37	0.18	0.14	0.55	0.06	0.14
	α	5.08	2.81	4.87	1.87	3.36	3.49
	R_S	4.77	1.25	6.35	3.39	1.99	4.20
	EEO	B < A	B < A	B < A	B < A	B < A	B < A
9	k_1	1.00	0.28	0.34	0.77	0.15	0.35
	α	9.11	5.13	44.85	5.63	3.27	4.06
	R_S	10.95	8.07	10.07	12.32	4.91	9.55
	EEO	B < A	B < A	B < A	B < A	B < A	B < A

Chromatographic conditions: columns, Phenomenex Lux Amylose-1 (coated, **cA1**) and i-Amylose-1 (**iA1**); mobile phase, 100% EtOH, 1-PrOH, 2-PrOH; flow rate, 1.0 mL min^{-1} (0.5 mL min^{-1} in 100% 1-PrOH and 2-PrOH); detection, 215 nm; temperature, 25 °C

Table A3. Effects of counterion concentration on the chromatographic parameters in the separation of **FBP** analytes applying ZIE CSPs

	Analyte		Mobile phase, MeOH containing DEA+FA (mM)				
			6.25+12.5	**12.5+25**	**25+50**	**50+100**	**100+200**
ZWIX(–)	**1**	k_1	3.77	3.10	2.82	2.35	1.73
		α	1.54	1.51	1.53	1.52	1.51
		R_S	2.97	2.88	3.15	2.99	3.06
	2	k_1	4.41	3.64	3.26	2.74	2.03
		α	1.49	1.47	1.49	1.48	1.50
		R_S	3.05	2.94	3.06	2.97	3.31
	Analyte		**Mobile phase, MeOH containing DEA+FA (mM)**				
			6.25+12.5	**12.5+25**	**25+50**	**50+100**	**100+200**
ZWIX(+)	**1**	k_1	3.70	3.19	2.70	2.05	1.42
		α	1.10	1.09	1.10	1.08	1.07
		R_S	0.90	0.88	0.94	0.71	0.52
	2	k_1	4.27	3.68	3.06	2.38	1.64
		α	1.11	1.11	1.13	1.09	1.08
		R_S	1.33	1.27	1.17	1.04	0.69

Chromatographic conditions: columns, ZWIX(–) and ZWIX(+); mobile phase, 100% MeOH containing DEA and FA; flow rate, 0.6 ml min^{-1}; detection, 262 nm; temperature, 25 °C

Table A4. Effects of additives in PIM on the chromatographic parameters in the enantioseparation of **ABA** analytes applying **cA1** CSP

Analyte		Mobile phase, EtOH Additives				
		–	0.1% DEA	0.1% DEA eq. FA	0.1% DEA 2eq. FA	eq. FA
1	k_1	0.66	0.70	0.70	0.70	0.55
	α	1.99	2.13	2.12	2.11	1.79
	R_S	7.73	8.98	8.58	8.64	1.62
	EEO	A < B	A < B	A < B	A < B	A < B
8	k_1	0.37	0.32	0.33	0.31	0.13
	α	5.08	6.78	6.60	6.72	5.05
	R_S	4.77	5.10	5.07	5.00	1.83
	EEO	B < A	B < A	B < A	B < A	B < A
12	k_1	0.59	0.64	0.65	0.65	0.48
	α	1.87	1.94	1.92	1.92	1.94
	R_S	1.92	1.88	1.85	1.84	1.75
	EEO	B < A	B < A	B < A	B < A	B < A

Chromatographic conditions: column, Phenomenex Lux Amylose-1; mobile phase, 100% EtOH; additives, none, 0.1 *v*% DEA, 0.1 *v*% DEA + eq. FA, 0.1 *v*% DEA + 2eq. FA, eq. FA, ("eq." = molar equivalent amount of FA with 0.1% DEA = 9.7 mM); flow rate, 1.0 ml min^{-1}; detection, 205–230 nm; temperature, 25 °C

Table A5. Effects of polarity (log P) and volume of the molecule (Å^3) on retention factor (k^1) in the enantioseparation of **ATO–1–9** analytes applying PS-based CSPs in NPM.

Analyte		k_1			
	log P	**IA**	**IB**	**IE**	**IC**
4	1.45	1.41	0.68	1.97	1.43
6	1.67	1.85	0.70	2.00	1.95
5	2.54	2.03	0.72	2.00	1.71
1	2.91	2.39	0.81	3.34	2.28
3	3.13	1.95	0.76	1.80	2.15
2	4.00	2.08	0.72	1.86	2.04
7	3.70	1.29	0.35	1.44	0.57
9	3.85	1.86	0.46	1.48	0.85
8	4.56	1.90	0.47	1.57	0.79
	Å^3	**IA**	**IB**	**IE**	**IC**
1	276	2.39	0.81	3.34	2.28
4	292	1.41	0.68	1.97	1.43
7	380	1.29	0.35	1.44	0.57
2	270	2.08	0.72	1.86	2.04
5	299	2.03	0.72	2.00	1.71
8	387	1.90	0.47	1.57	0.79
3	266	1.95	0.76	1.80	2.15
6	290	1.85	0.70	2.00	1.95
9	377	1.86	0.46	1.48	0.85

Chromatographic conditions: columns, Chiralpak IA, IB, IE, and IC; mobile phase, *n*-hexane/EtOH 80/20 (*v/v*); flow rate, 1.0 mL min^{-1}; detection, 220 nm; temperature, 25 °C. The data had categorized into groups of three based on the structural characteristics of the analytes and lined up by increasing polarity or volume.

Table A6. Effect of temperature on chromatographic parameters k_1, α and R_S in the enantioseparation of **FBP** analytes applying **ZWIX(+)** CSP

Analyte		5 °C		10 °C		20 °C		30 °C		40 °C		50 °C	
		a	**b**	**a**	**b**	**a**	**b**	**a**	**b**	**a**	**b**	**a**	**b**
1	k_1	3.23	7.24	3.12	6.64	2.81	5.94	2.55	5.51	2.24	4.91	2.03	4.48
	α	1.10	1.27	1.10	1.25	1.09	1.22	1.08	1.19	1.07	1.17	1.07	1.15
	R_S	0.91	2.58	0.92	2.59	0.87	2.46	0.81	2.24	0.76	1.86	0.64	1.37
2	k_1	3.76	8.05	3.51	7.39	3.23	6.59	2.88	6.06	2.51	5.35	2.34	4.82
	α	1.12	1.28	1.11	1.26	1.10	1.23	1.09	1.20	1.08	1.17	1.07	1.15
	R_S	1.14	2.74	1.07	2.58	1.07	2.62	0.88	2.31	0.79	1.87	0.56	1.29
3	k_1	4.35	9.21	3.94	8.35	3.58	7.38	3.18	6.66	2.78	5.78	2.55	5.07
	α	1.13	1.29	1.12	1.27	1.10	1.23	1.08	1.20	1.07	1.17	1.06	1.15
	R_S	1.15	2.75	1.06	2.53	0.94	2.39	0.85	2.17	0.76	1.80	0.45	1.14
4	k_1	3.91	8.83	3.61	7.98	3.38	7.01	2.91	6.23	2.53	5.32	2.35	4.60
	α	1.11	1.30	1.10	1.28	1.08	1.24	1.07	1.20	1.05	1.17	1.04	1.15
	R_S	1.03	2.82	1.00	2.73	0.97	2.57	0.68	2.22	0.60	1.84	0.27	0.98
5	k_1	2.87	6.76	2.67	6.08	2.58	5.47	2.23	4.99	1.97	4.38	1.84	4.02
	α	1.20	1.33	1.19	1.31	1.18	1.28	1.16	1.25	1.15	1.22	1.14	1.19
	R_S	1.66	2.85	1.55	2.60	1.82	2.73	1.41	2.57	1.43	2.08	1.03	1.29
6	k_1	3.90	8.85	3.57	7.84	3.22	6.64	2.80	5.65	2.36	4.60	2.08	3.78
	α	1.08	1.16	1.08	1.16	1.08	1.15	1.08	1.14	1.08	1.13	1.07	1.11
	R_S	0.85	1.78	0.83	1.77	0.87	1.83	0.86	1.78	0.85	1.37	0.57	0.42

Chromatographic conditions: column, ZWIX(+); mobile phase, all containing 25 mM DEA and 50 mM FA, **a)** MeOH; flow rate, 0.6 mL min^{-1}, **b)** MeOH/MeCN 50/50 (*v/v*); flow rate, 0.6 mL min^{-1}; detection, 262 nm; temperature, 5–50 °C

Table A7. Effects of eluent composition on the thermodynamic parameters in the separation of **FBP** analytes applying **ZWIX(+)** CSP

Analyte	$-\Delta(\Delta H^0)$ (kJ mol^{-1})		$-\Delta(\Delta S^0)$ (J mol^{-1} K^{-1})	
	a	**b**	**a**	**b**
1	0.54 ± 0.03	1.69 ± 0.08	1.12 ± 0.09	4.07 ± 0.27
2	0.73 ± 0.03	1.78 ± 0.10	1.70 ± 0.10	4.36 ± 0.34
3	1.09 ± 0.07	1.96 ± 0.11	2.93 ± 0.25	4.95 ± 0.38
4	1.13 ± 0.07	2.11 ± 0.12	3.18 ± 0.25	5.39 ± 0.41
5	0.86 ± 0.06	1.86 ± 0.05	1.60 ± 0.19	4.30 ± 0.17
6	-	0.75 ± 0.20	-	1.39 ± 0.68
	$-\Delta(\Delta G^0)_{298K}$ (kJ mol^{-1})		$Q = \Delta(\Delta H^0) / [T^*\Delta(\Delta S^0)]$	
1	0.20 ± 0.04	0.47 ± 0.11	1.61 ± 0.15	1.39 ± 0.11
2	0.22 ± 0.04	0.48 ± 0.14	1.43 ± 0.11	1.37 ± 0.13
3	0.22 ± 0.10	0.49 ± 0.16	1.25 ± 0.14	1.33 ± 0.13
4	0.18 ± 0.11	0.50 ± 0.17	1.19 ± 0.12	1.31 ± 0.13
5	0.38 ± 0.08	0.58 ± 0.07	1.81 ± 0.24	1.45 ± 0.07
6	-	0.33 ± 0.28	-	1.80 ± 0.44

Chromatographic conditions: column, ZWIX(+); mobile phase, **a)** MeOH; **b)** MeOH/MeCN 50/50 (*v/v*) all containing 25 mM DEA and 50 mM FA; flow rate, 0.6 mL min^{-1}; detection, 262 nm.

Table A8. Thermodynamic parameters, $\Delta(\Delta H^0)$, $\Delta(\Delta S^0)$, $\Delta(\Delta G^0)$, and *Q* values of **ATO** analytes on the cellulose-based **IB** and **IC** columns.

Analyte	$-\Delta(\Delta H^0)$ (kJ mol^{-1})	$-\Delta(\Delta S^0)$ (J mol^{-1} K^{-1})	$-\Delta(\Delta G^0)_{298K}$ (kJ mol^{-1})	Q
	Column: **IB**			
1	0.78 ± 0.16	1.92 ± 0.53	0.20 ± 0.23	1.36 ± 0.47
2	2.04*	6.96*	0.04*	0.98*
3	0.71 ± 0.23	1.42 ± 0.78	0.29 ± 0.33	1.68 ± 1.07
4	n.s.	n.s.	n.s.	n.s.
5	-2.73 ± 0.31	-9.63 ± 1.04	0.15 ± 0.44	0.95 ± 0.15
6	0.66 ± 0.17	1.24 ± 0.56	0.29 ± 0.24	1.78 ± 0.93
7	1.30 ± 0.22	3.06 ± 0.74	0.39 ± 0.31	1.42 ± 0.42
8	0.98 ± 0.28	1.99 ± 0.92	0.39 ± 0.39	1.65 ± 0.90
9	1.19 ± 0.20	2.75 ± 0.66	0.37 ± 0.28	1.45 ± 0.42
10	1.63 ± 0.42	4.78 ± 1.45	0.20 ± 0.60	1.14 ± 0.46
	Column: **IC**			
1	0.79 ± 0.25	1.21 ± 0.82	0.43 ± 0.35	2.19 ± 1.65
2	-1.35 ± 0.24	-4.63 ± 0.79	0.03 ± 0.34	0.98 ± 0.24
3	2.19 ± 0.20	4.66 ± 0.64	0.80 ± 2.27	1.58 ± 0.26
4	4.22 ± 0.29	10.86 ± 0.96	0.98 ± 0.41	1.30 ± 0.15
5	5.38 ± 0.24	14.34 ± 0.81	1.11 ± 0.34	1.26 ± 0.09
6	5.02 ± 0.19	13.16 ± 0.65	1.09 ± 0.27	1.28 ± 0.08
7	-1.33 ± 0.24	-5.56 ± 0.80	0.32 ± 0.34	0.81 ± 0.19
8	1.45 ± 0.10	3.40 ± 0.34	0.44 ± 0.14	1.43 ± 0.17
9	n.s.	n.s.	n.s.	n.s.
10	8.40 ± 0.20	22.32 ± 0.68	1.74 ± 0.28	1.26 ± 0.05

Chromatographic conditions: column, Chiralak IB and IC; mobile phase, *n*-hexane/EtOH/DEA 80/20/0.1 (*v/v/v*); flow rate, 1.0 mL min^{-1}; detection, 220 nm; temperature, 10–50°C. $Q = \Delta(\Delta H^0) / [T^*\Delta(\Delta S^0)]$. n.s.: no separation observed. *: not enough data points (a.k.a. enantioseparations) in the temperature range to calculate confidence intervals.

Table A9. Relative standard deviations of the chromatographic parameters calculated from three consecutive measurements of three different analytes in three different mobile phase systems in the enantioseparation of **ABA** analytes

Eluent and analyte		k_1	k_2	α
a) **1**	mean	0.572	2.286	3.999
	SD	0.00191	0.00876	0.00378
	RSD (%)	**0.346**	**0.428**	**0.102**
b) **6**	mean	1.431	1.614	1.130
	SD	0.00622	0.00135	0.00422
	RSD (%)	**0.447**	**0.083**	**0.364**
b) **12**	mean	0.509	1.168	2.294
	SD	0.00089	0.00185	0.00702
	RSD (%)	**0.168**	**0.164**	**0.329**
c) **1**	mean	0.196	0.347	1.772
	SD	0.00179	0.00187	0.00463
	RSD (%)	**0.760**	**0.481**	**0.280**

Chromatographic conditions: column, Phenomenex Lux Amylose-1; mobile phase, a) 100% MeOH, b) 2-PrOH/MeOH 40/60 (*v/v*), c) 100% 2-PrOH, flow rate, 0.5 ml min^{-1}; detection, 215 nm; temperature, 25 °C

The contribution ratio of each enantiomer (r_A and r_B) to the hysteresis were calculated from the hystereticity factors as the following equation shows:

$$r_A = \frac{|\log(\nu_A)|}{|\log(\nu_A/\nu_B)|} \tag{10}$$

The r_B ratios were calculated analogously as in **Eq. (10)**. Calculation of the percentage contributions of the enantiomers ($\%_A$ and $\%_B$) to the hysteresis were made as the next equation describes:

$$\%_A = \frac{r_A}{r_A + r_B} \times 100 \tag{11}$$

The $\%_B$ values were calculated analogously as in **Eq. (11)**.

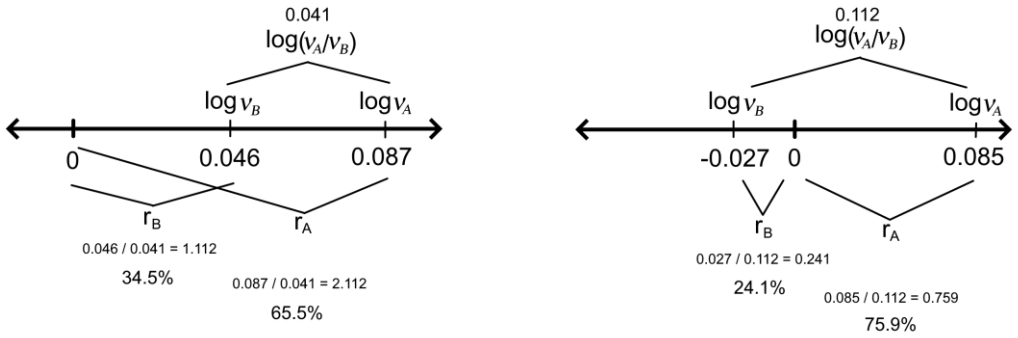

Figure A2. Two simple examples for the easier understanding of the hysteresis-related parameters. The hystereticity factor (ν) of the A and B enantiomers are changed parallel on the left (**ABA–7** from **Table A10**, 80/20 column) and the opposite way on the right (**ABA–8** from **Table A10**, 80/20 column).

Table A10. Effects of hysteresis on the selectivity (defined based on the configuration) and percentage contribution of a single enantiomer to the overall hysteresis in the separation of all **ABA** analytes applying **cA1** CSP

Analyte	Mobile phase, 2-PrOH/MeOH (*v/v*)							
	80/20		60/40		40/60		20/80	
	$\log(v_A/v_B)$	$\%_A$	$\log(v_A/v_B)$	$\%_A$	$\log(v_A/v_B)$	$\%_A$	$\log(v_A/v_B)$	$\%_A$
1	0.003	84.7	-0.054	17.6	0.146	35.6	0.011	9.2
2	0.009	93.7	0.038	59.9	0.181	57.4	0.012	11.0
3	0.005	64.9	0.000	50.4	0.021	35.9	0.004	28.1
4	-0.010	47.7	0.005	64.8	0.043	69.9	0.004	3.9
5	0.010	51.8	0.005	60.0	0.016	20.3	0.000	53.7
6	0.001	50.6	-0.002	40.3	0.099	10.2	0.000	50.6
7	0.041	65.5	-0.006	34.3	-0.011	40.5	-0.002	58.6
8	0.112	75.9	0.085	36.2	-0.112	97.1	-0.006	78.1
9	0.439	88.9	0.010	58.3	-0.281	97.0	-0.015	86.0
10	-0.115	32.3	0.008	91.6	-0.258	66.4	0.000	48.6
11	0.268	96.7	0.042	43.8	-0.236	97.9	-0.008	71.9
12	0.014	19.1	0.021	31.9	-0.165	48.6	-0.004	61.8
13	0.026	67.7	0.004	28.1	-0.235	73.7	-0.009	78.8

Chromatographic conditions: column, Phenomenex Lux Amylose-1; mobile phase, 2-PrOH/MeOH, flow rate, 0.5 ml min^{-1}; detection, 205–215 nm; temperature, 25 °C. Negative values indicate the selectivity (based on the configuration) were higher when measured from the direction of 2-PrOH (forward). The calculated approximate confidence interval of the phenomenon of hysteresis of selectivity (a.k.a. $\log(v_A/v_B)$ data) is 0 ± 0.0122. The results that fall inside of this confidence interval are black in the table; **grey** numbers indicate that there is no significant hysteresis on the selectivity (defined based on the configuration) observed in these cases.